Attenuation of mammary gland dysplasia and feeding difficulties in *Tabby* mice by fetal therapy

Mandy Wahlbuhl[1#], Sonia Schuepbach-Mallepell[2], Christine Kowalczyk-Quintas[2], Angela Dick[1], Fabian B. Fahlbusch[1], Pascal Schneider[2], Holm Schneider[1]

[1]Department of Pediatrics and Adolescent Medicine, Friedrich-Alexander University Erlangen-Nuremberg, Germany, [2]Department of Biochemistry, University of Lausanne, Epalinges, Switzerland

[#]Corresponding author:

Dr. Mandy Wahlbuhl-Becker
Department of Pediatrics and Adolescent Medicine
Friedrich-Alexander University Erlangen-Nuremberg
Loschgestr. 15
91054 Erlangen
Germany
Phone: +49 9131 85 41277, Fax: +49 9131 85 36224
E-mail: mandy.wahlbuhl-becker@uk-erlangen.de

Abstract

Hypohidrotic ectodermal dysplasias (HED) are hereditary differentiation disorders of multiple ectodermal structures including the mammary gland. The X-linked form of HED (XLHED) is caused by a lack of the secreted signaling molecule ectodysplasin A1 (EDA1) which is encoded by the gene *EDA* and belongs to the tumor necrosis factor (TNF) superfamily. Although male patients (hemizygous) are usually more severely affected by XLHED, heterozygous female carriers of an *EDA* mutation may also suffer from a variety of symptoms, in particular from abnormal development of their breasts. In *Tabby* mice, a well-studied animal model of XLHED, EDA1 is absent. We investigated the effects of prenatal administration of Fc-EDA, a recombinant EDA1 replacement protein, on mammary gland development in female *Tabby* mice. Intra-amniotic delivery of Fc-EDA to fetal animals resulted later in improved breastfeeding and thus promoted the growth of their offspring. In detail, such treatment led to a normalization of the nipple shape (protrusion, tapering) that facilitated sucking. Mammary glands of treated female *Tabby* mice also showed internal changes, including enhanced branching morphogenesis and ductal elongation. Our findings indicate that EDA receptor stimulation during development has a stable impact on later stages of mammary gland differentiation, including lactation, but also show that intra-amniotic administration of an EDA1 replacement protein to fetal *Tabby* mice partially corrects the mammary gland phenotype in female adult animals.

Introduction

Ectodermal dysplasias are a group of rare and heterogeneous hereditary disorders, characterized by impaired development of multiple ectodermal structures such as hair, nails, teeth, and various eccrine glands including sweat and mammary glands [1, 2]. X-linked hypohidrotic ectodermal dysplasia (XLHED; Christ-Siemens-Touraine syndrome; #MIM 305100), the most frequent of the numerous ectodermal dysplasias, is caused by mutations in the gene *EDA* (located on chromosome Xq12–q13.1), which encodes ectodysplasin A1 (EDA1, hereinafter EDA), a member of the tumor necrosis factor ligands family. XLHED is a rare disorder with an incidence between 1:30000 and 1:100000. Mutations in the genes coding for the EDA receptor (*EDAR* on chromosome 2q11–q13) and its associated death domain-containing adaptor protein (*EDARADD* on chromosome 1q42–q43) result in autosomal dominant (#MIM 129490) and autosomal recessive (#MIM 224900) forms of HED [3]. The proteins encoded by these three genes are all involved in the common nuclear factor (NF)-κB signaling pathway which is fundamental for normal ectodermal development and a key mediator of EDA signaling [4]. A few potential target genes of the EDA-NF-κB pathway have been identified. These include *CCND1* [5], *DKK4* [6], *PTHrP*, *WNT10a*, and *WNT10b* as well as the EGF family ligand genes *AREG* and *EPGN* [7]. Moreover, EDA has been identified as a factor influencing different steps of mammary gland morphogenesis through activation of NF-κB signaling in the epithelium [7]. Mutations in *EDA*, *EDAR* and *EDARADD* lead to similar phenotypes. Male XLHED patients (hemizygous for an *EDA* mutation) are more severely affected than heterozygous female carriers who present with variable symptoms such as missing and/or abnormal teeth, hypotrichosis and a reduced ability to sweat (hypohidrosis) [8-10]. Many affected women also suffer from an abnormal development of their breasts. Beyond the individual cosmetic relevance, this can severely limit their breastfeeding ability [11]. Various case reports have documented a disruption of breast development secondary to mutations in one of the genes of the EDA signaling pathway in humans [12-16].

Development of the mammary gland starts in the fetus. Sequential and reciprocal signals between the epithelium and surrounding mesenchyme implement the outgrowth of a small duct into the dermal mesenchyme and formation of the nipple. During puberty the cyclical production of hormones accelerates ductal outgrowth and branching. Proliferation and maturation of the alveolar compartment occurs only during pregnancy. At term, the breasts reach maturity and produce milk to feed the young [17].

Tabby mice represent a well-studied animal model of XLHED [18-20] in which the EDA protein is absent due to a deletion of exon 1 [8]. Prenatal intravenous administration of Fc-EDA, a recombinant fusion protein consisting of the receptor-binding domain of EDA and the Fc part of immunoglobulin G1, to pregnant dams corrected the developmental abnormalities in the offspring [21]. This treatment strategy, however, exposes the mother to high serum levels of an exogenous molecule and may be suboptimal for achieving reproducible drug concentrations in human fetuses. Therefore, fetal *Tabby* mice were treated by intra-amniotic administration of Fc-EDA, which resulted in a complete reversion of the XLHED phenotype [22] including normalized eye opening, retro-auricular and guard hair growth, and regular eccrine sweat gland function at the paws. In addition, size and shape of the molars resembled those of wild-type mice [22].

Here we report an improvement of the breastfeeding ability of female *Tabby* mice following prenatal treatment with Fc-EDA. Intra-amniotic administration of this replacement protein to fetuses partially corrected mammary gland development including the nipple shape in female animals, while epithelial function was not completely restored.

Material and methods

Animal model and treatment

C57BL/6 wild-type mice (Charles River, Sulzfeld, Germany), white-bellied agouti B6CBAa *Aw-J/A-EdaTa*/J *Tabby* mice (000314; Jackson Laboratory, Bar Harbor, USA) and appropriate control mice were housed in individually ventilated cages under standard conditions with a light/dark cycle of 12 hours and free access to standard chow and tap water. All experimental procedures on animals were conducted in accordance with the German regulations and legal requirements and had been approved by the local government authorities. Intra-amniotic injections were performed as described previously [22]. In short, time-mated pregnant mice on gestational day 15 (E15) were anesthetized with isoflurane (2%). For perioperative analgesia, metamizole (100 µl, 50 mg/ml) was administered subcutaneously. The abdominal cavity was opened by midline laparotomy and both uterine horns were exposed completely. Fc-EDA was injected into the amniotic sacs of individual fetuses at doses of 100 µg/g fetal body weight (16 µl of Fc-EDA at 2.2 mg/ml, assuming a fetal weight of approximately 0.35 g) using glass syringes with 33 gauge needles (Hamilton Robotics, Bonaduz, Switzerland). The uterus was then placed back in the abdomen, the abdominal wall was closed by continuous suture of the peritoneal layer and interrupted stitches of the skin, and mice were allowed to recover in a pre-warmed cage.

All treated fetuses survived the injection procedure and were born without complications. For breastfeeding studies untreated and prenatally Fc-EDA-treated *Tabby* females were time-

mated with male *Tabby* mice. Wild-type matings served as controls. Around day 18.5 of gestation, the cages were checked daily for new litters. The day of birth is defined as day P0 and the litter size was recorded. The pups were weighed daily and their size was measured at P0, P10 and P20. The sex was recorded at day 17. When wild-type and *Tabby* litters were born on the same day, a litter exchange (with about half of the litter) was done. According to the age at analysis, P0, P21, P42 or lactating day 1 (L1), the mice were sacrificed by decapitation (P0) or cervical dislocation (other time points) and inguinal mammary glands were harvested as described elsewhere [23]. For macroscopic analysis of nipple development, digital close-up pictures were taken and scored (i.e. *1,* flat nipple; *2,* cubical form; *3,* cylindrical shape). Representative examples are displayed in Supplementary Figure 2.

Carmine Alum Staining

For whole mount analysis the 4th inguinal glands were spread on glass slides, fixed overnight in glacial acetic acid/ethanol (2:8, v/v), rehydrated through descending alcohol series, and stained with carmine alum (Sigma-Aldrich, Taufkirchen, Germany) overnight. Stained tissues were dehydrated and soaked with BABB (Benzylalcohol : Benzylbenzoate 1:2; Sigma-Aldrich). Whole mount mammary glands were subsequently investigated using a Leica stereomicroscope MZ 10F (Leica Microsystems, Wetzlar, Germany) with Zeiss Axiocam Typ MRc and Axiovision 4.7 software (Carl Zeiss Microscopy GmbH, Göttingen, Germany). Quantification of the fat pad area filled by ducts was performed via ImageJ software [24] as described elsewhere [25]. The peripheries of the gland and of the ductal tree were contoured manually and the respective pixel areas were recorded digitally. The ratio of these two areas (Fig. 4 d-f) represents the percentage of fat pad area filled by ducts.

Immunohistochemistry

Mammary tissues of untreated or Fc-EDA-treated *Tabby* and wild-type female mice were fixed in 4% PFA overnight, embedded in paraffin, and cut into 5-µm sections. Dewaxed and rehydrated sections were stained with hematoxylin-eosin for quantification of the epithelial content. To prepare sections for immunofluorescence staining they were heated in a microwave oven (650W) for 15 minutes in sodium citrate buffer (pH 9.0 for ZO-1, occludin, E-cadherin, PCNA; pH 6.0 for Krt14, SMA, except for the fluorescent milk proteins staining where no antigen retrieval was required). Sections were blocked using 10% normal goat serum in protein block solution (DAKO, Hamburg, Germany) and incubated overnight with primary rabbit antibodies against ZO-1 and occludin (1:50 and 1:100, respectively; Thermo Fisher, Schwerte, Germany) or Keratin 14 (1:50; Biolegend, Koblenz, Germany), mouse antibodies against SMA (1:500; Sigma-Aldrich), PCNA (1:200; DAKO Hamburg, Germany) or

E-cadherin-FITC (1:100; BD Bioscience, Heidelberg, Germany) and rabbit anti-milk serum (1:5000; Accurate Chemical, Westbury, USA), followed by secondary Alexa fluor 594-labelled goat anti-rabbit or anti-mouse (1:500; Thermo Fisher) or Alexa fluor 488-labelled goat anti-mouse (1:500; Thermo Fisher) antibodies, diluted in blocking solution. Sections were analyzed using the Axiovert 200M microscope and the AxioVision software (Carl Zeiss Microscopy GmbH). Quantification was performed with ImageJ software [24]. The number of epithelial PCNA-positive cell nuclei and TUNEL-positive cells was normalized to the total number of DAPI-positive cells per duct, respectively.

Sudan III lipid staining

Lipids in L1 glands were visualized by Sudan III staining. Cryosections were fixed in 4% PFA for 30 minutes, washed with 50% ethanol, stained with 0.3% Sudan III solution (Merck Millipore, Billerica, Massachusetts, USA) in 70% ethanol for 25 minutes and then washed with 50% ethanol. Subsequently, slides were counterstained with hemalum.

Western blotting

Western blotting was performed according to standard procedures as described previously [26]. Snap-frozen 4th inguinal mammary glands at L1 were homogenized and lyzed using cell lysis buffer (50 mM Tris pH 7.4, 150 mM Sodium chloride, 1% Nonident P40, 0.25% Sodiumdesoxycholat, 1 mM EDTA, 1mM PMSF, 1 mM Sodium fluoride, 1μg/ml Aprotinin, Leupeptine, Pepstatin). After centrifugation supernatants were stored at -20°C. Protein concentrations were measured using the BCA assay and 20 μg of each sample were separated on a 10% SDS gel. Rabbit anti-milk serum (1:1000; Accurate Chemical, Westbury, USA) was used as primary antibody, and for loading control rabbit anti-GAPDH, followed by HRP-conjugated anti-rabbit antibody (1:500; Cell Signaling Technology, Leiden, The Netherlands) as secondary antibody. Amersham ECL Western Blotting detection reagent (GE Healthcare Life Sciences, Freiburg, Germany) and the ADVANCED Fluorescence and ECL imager (INTAS science imaging, Göttingen, Germany) were used for detection. Densitometric estimation of the relative amount of protein normalized to GAPDH was performed with ImageJ software [24] as described elsewhere [25].

RNA isolation and qPCR

Total *RNA* from the 4th inguinal mammary glands at L1 was extracted with *TRIzol* (Thermo Fisher) and reverse transcription was performed using the ThermoScript RT-PCR System (Thermo Fisher). For real-time PCR with a SYBR-green-based RT-PCR assay on the CFX96 Touch™ Real-Time PCR Detection System (BioRad, München, Germany), the following specific primer sequences were used: EDA_forward) GCAGGCCGTCCTTTCAACG;

EDA_reverse CTTCAGAATATGCCTTTTCATCA; E-Cad_forward GCAGGCCGTCCTTTCAACG; E-Cad_reverse TCCAAATCCGATACGTGATCTTC; ß-Actin_forward ATGCTCCCCGGGCTGTAT; ß-Actin_reverse TCACCCACATAGGAGTCCTTCTG; ZO-1_forward GAGAAGCTGGATTCCTAA; ZO-1_reverse TCTCGZGGTTCACTTTTTGCA; SMA_ forward CTGACGGGCAGGTGATCAC; SMA_reverse GATGCCCGCTGACTCCAT; K14_forward TGAGAGCCTCAAGGAGGAGC; K14_reverse TCTCCACATTGACGTCTCCAC; ß-casein_forward GCTGCAGGCAGAGGATGTG; ß-casein _reverse GTTTGAGCCTGAGCATATGGAAA; WAP_forward TGTCCCGGTACCTGTGGTA; WAP_reverse GGCAGAAGCCAGCTTTCG; Ccdn1_forward ACGCACTTTCTTTCCAGAGTCAT; Ccdn1_reverse CTCCAGAAGGGCTTCAATCTGT; Elf5_forward GCTGATTCCAGTTGCTTGAAAAC; Elf5_reverse GGGACAGCAGCAAGTCTCTGA; RANKL_forward GGTCTAACCCCTGGACATGTG; RANKL_reverse CTTTGCAATGACATGGCATCCT; RANK_forward CGAGGAAGATTCCCACAGAG; RANK_reverse CAGTGAAGTCACAGCCCTCA; PGR_forward GGTCCCCCTTGCTTGCA; PGR_reverse CAGGACCGAGGAAAAAGCAG; PRLR_forward GCAGTGGCTTTGAAGGGTTA; PGLR_reverse TGCTAGAGAAGGGCAAGTCTG; ESR1_forward TTCGTCCAGCACCTTGAAGTCTCTG, ESR1_reverse CATCTCCAGGAGCAGGTCATAGAGG. Gene expression was normalized to E-cadherin (epithelial marker [34]) and ß-actin housekeeping genes and analyzed by the comparative cycle threshold method (ΔΔCt).

Statistical Analysis

Statistical analysis was performed using the GraphPad Prism software 7 (GraphPad Software Inc., La Jolla, USA). Unpaired t-tests were used for the comparison of two samples and one-way ANOVA with Bonferroni's multiple comparison test for multiple samples. Data are shown as mean ±SEM, unless stated otherwise.

Results

Inadequate weight gain of neonatal *Tabby* mice depends on the mother

Due to the lack of EDA protein, the *Tabby* mouse strain exhibits a phenotype characterized by abnormally shaped teeth, missing sweat glands and absence of certain hair types [18, 27]. In addition, growth restriction is conceived to be a feature of *Tabby* mice, yet no conclusive data have been published so far. Therefore our litters were weighed daily from the date of birth (P0) to weaning (P20). After birth, body weights of mice steadily increased for more than two weeks and then stabilized between P16 and P18 (Fig. 1a). Hence, P17 was chosen to compare the weight of several hundreds of wild-type and *Tabby* pups (Fig. 1b). Although growth and weight gain varied considerably between litters especially in *Tabby* mice (Fig. 1a), the mean weight of *Tabby* pups was significantly lower (7.0±1.2 g) than that of wild-type pups (7.5±1.0 g) at P17 (Fig. 1b). Additionally, the mean weight of pups depended on the litter size both in wild-type and *Tabby* mice: mice from small litters were up to one gram heavier than those from large litters (Fig. 1c). No sex-specific weight differences were observed at that age (Fig. 1d).

To elucidate the cause of growth restriction in our animal model, cross-fostering was performed. When wild-type and untreated *Tabby* litters were mixed at P1 and subsequently re-distributed to *Tabby* or wild-type dams, *Tabby* pups fed by wild-type dams had the same mean weight as wild-type pups fed by wild-type dams (Fig. 1e). Furthermore, wild-type pups fed by untreated *Tabby* dams showed the same mean weight as untreated *Tabby* pups fed by untreated *Tabby* dams (Fig. 1e). These results indicate that the postnatal growth restriction of untreated *Tabby* pups is a result of EDA-deficiency in mothers, but not in the pups themselves.

Corrected nipple anatomy in *Tabby* females following prenatal treatment with Fc-EDA

The mammary gland is composed of a complex ductal tree that converges into a central duct at the nipple. During pregnancy, nipples undergo changes in size and architecture. During the first half of pregnancy nipples acquire a conical shape, in the second half (days 15 to 18 in the mouse) their size increases [28]. Nipple shape and functionality are important prerequisites for breastfeeding. Macroscopic comparison of native *Tabby* and wild-type nipples on day 1 of lactation (L1) with a scoring system revealed that the nipples of untreated *Tabby* mice had significant morphological deficits (Fig. 2a, d) when compared with treated *Tabby* mice or wild-type dams (p<0.05 and p<0.01, respectively). Their nipples appeared smaller and flattened rather than cylindrical as in wild-type animals (Fig. 2c, d). Nevertheless, the pups of untreated *Tabby* dams were able to suckle after birth. Prenatal treatment with Fc-

EDA on E15 increased the height and tapering of nipples in adult *Tabby* mice (Fig. 2b, d) towards those of wild-type mice (Fig. 2c, d).

Improved breastfeeding ability and behavior of *Tabby* mice treated with Fc-EDA

Next, we investigated whether prenatal treatment with Fc-EDA would improve the maternal breastfeeding capacity during the phase of lactation in later life, comparing the weight of pups from Fc-EDA-treated and control mothers (Fig. 3a-c). The body lengths of these pups were measured at P0, P10 and P20. The sex was determined at P17. Breastfeeding was analyzed in litters of defined size (5–7 pups) and was compared between Fc-EDA-treated *Tabby* mothers, untreated *Tabby* and wild-type mice (Fig. 3a). While all three groups had similar birth weights and BMI (not shown), the pups of Fc-EDA-treated mothers gained significantly more weight (p<0.001) when breastfed than pups of untreated mothers (Fig. 3b). As a consequence, the pups of Fc-EDA-treated mothers were significantly heavier (11%, p<0.001) than pups of untreated mothers at P20 (Fig. 3a). Pups of Fc-EDA-treated mothers also showed a significantly higher BMI at P10 (Fig. 3b) but similar longitudinal growth. In none of the groups, sex-linked weight differences were observed at birth or at P17 (Fig. 3c).

Enhanced branching morphogenesis in treated mammary glands during development

The prenatal administration of Fc-EDA improved branching morphogenesis and ductal elongation in *Tabby* mice when compared with mammary gland development of untreated *Tabby* females (Fig. 4). In Fc-EDA-treated pups, a ductal tree with about 12±1 branches had formed in the mammary gland at P0. At the same time point, mammary glands of untreated *Tabby* mice displayed significantly less end tips (6.6±0.5, p<0.05, Fig. 4g) and branch points (6.0±0.8 vs. 9.0±2.0, p<0.05, Fig. 4h) in whole mount sections. At the prepubertal stage (P21) and during puberty (P42) branching morphogenesis and ductal elongation in Fc-EDA-treated *Tabby* mice remained superior to their untreated counterparts (Fig. 4), with a marked increase in the number of end tips (4.8±2.0 vs. 15.5±1.5 at P21, p<0.05, Fig. 4g) and branch points (7.6±0.8 vs. 13.5±0.5, p<0.05, Fig. 4h) at P21. The effect of Fc-EDA treatment on mammary gland branching morphogenesis was evident also at P42 (Fig. 4a-f), when 2.3-fold more end tips (56.0±8.0) were found in treated mammary glands (Fig. 4b, e, g) than in glands from untreated *Tabby* mice (24.0±2.5; Fig. 4a, d, g). As elongation of mammary ducts in mice takes place as a result of rapid growth of their end buds and depends on branching, the number of branching points is considered a valid proxy for the outgrowth of the ducts [29]. At P42 we found a ~3-fold increase in the number of branch points when comparing untreated with Fc-EDA-treated *Tabby* mice (14.6±1.8 vs. 42.3±10.7, respectively; p<0.001, Fig. 4h). Our whole mount histology additionally showed that mammary glands of untreated *Tabby* mice (Fig. 4a, d, g-i) remained poorly developed throughout the observational period,

with a much smaller area of fat pad filled by epithelial structures at P21 (1.4±0.8 vs. 4.5±0.3, p< 0.05, Fig. 4d, i) and P42 (8.9±1.5 vs. 25.0±8.3, p< 0.05, Fig. 4d, i) than in wild-type mice.

Significant effects of prenatal Fc-EDA treatment on alveologenesis

As analysis during puberty indicated a significant effect of Fc-EDA treatment on mammary gland branching morphogenesis and pups from untreated *Tabby* mothers showed slower weight gain than pups from Fc-EDA-treated mothers, we further hypothesized that Fc-EDA might also have beneficial long-term effects on mammary gland development during alveolo- (E14.5 and E18.5) and lactogenesis (L1). At mid-pregnancy alveoli divide and alveolar cells form an envelope surrounding the circular lumen. Thus, the epithelial cell number and epithelial surface area increase [30]. At the end of pregnancy we observed >20% epithelial structures in the mammary fad pad (Fig. 5c, g), compared to ~5% pre-gestationally.

While epithelial ducts of *Tabby* mice undergo alveolar switching (Fig. 5a), their extension into the mammary fat pad remained insignificant throughout gestation (~12% at all time points investigated, Fig. 5g). Interestingly, Fc-EDA treatment increased the gestational alveolar growth by up to 27%, so that ~16% of the fat pad were occupied by alveoli (Fig. 5b, g) at L1. Treatment with Fc-EDA, however, did not lead to a complete normalization of alveologenesis when compared with wild-type mice (Fig. 5c, g). Nevertheless, the improvement was sufficient to support the postnatal growth of pups (Fig. 3).

Reduced expansion of alveoli and the predominance of adipocytes in the mammary glands of untreated *Tabby* mice were clearly evident (Fig. 5a`, b`). The presence of large cytoplasmic lipid droplets (CLD) in untreated and Fc-EDA-treated mammary glands could be indicative of a secretory dysfunction [31, 32] in these mice (Fig. 5a`, b`). This illustrates that treatment with Fc-EDA does not lead to a complete rescue of mammary function, although the breastfeeding ability of treated mothers improved (Fig.3). We further investigated whether the observed effects of Fc-EDA on the mammary gland were secondary to enhanced proliferative or decreased apoptotic activities within epithelial structures. Immunofluorescence staining for PCNA *(*Proliferating Cell Nuclear Antigen) on mammary glands at an age of 6 weeks and at L1 revealed a significantly increased proliferation rate of epithelial cells at P42 and of alveolar cells at L1 in Fc-EDA-treated dams (Fig. 5d, e, f, h). In detail, the epithelial proliferation rate was approximately 40% and 15% higher at P42 and L1, respectively, (10.0±1,8 and 16.0±0.91) than in untreated animals (6.0±1.0 and 12.0±0.3). Analysis of ductal apoptosis via TUNEL assay showed no significant differences between untreated (5.0±0.8 and 2.4±0.3), Fc-EDA-treated (5.0±0.7 and 2.2±0.2) and wild-type (4.4±0.9 and 2.3±0.4) mice at the same time points (Fig. 5i), with a generally low percentage of TUNEL-positive cells. These findings suggest that the delay in mammary gland

development in untreated *Tabby* mice is at least partly due to reduced proliferation of their epithelial ducts.

To investigate the glandular architecture of secretory alveoli, mammary epithelia from untreated, Fc-EDA-treated and wild-type mammary glands, we performed immunofluorescence staining for proteins involved in cell-cell junctions (ZO-1, occludin, and E-cadherin [33, 34]) (Fig. 6a-c, Supplementary Fig. 3) and mammary basal cell markers (keratin 14 [35, 36] and alpha-smooth muscle actin (SMA) [35, 37]) (Fig. 6d-f). Our analysis revealed that the apical expression of ZO-1 seemed irregular in the epithelium of *Tabby* mammary glands independent of their Fc-EDA-treatment status (Fig. 6a, b). In contrast, marker proteins of glandular cell-cell adherence (E-cadherin, Fig. 6c, d), the major integral epithelial tight-junction protein occludin (Supplementary Fig. 3), basal cell structure and myoepithelial function of outer glandular cells (keratin 14 and SMA, Fig. 6c-e) were located as expected within the gland. The concomitant quantitative RT-PCR (qPCR) analysis of these genes showed no significant expression differences (Fig. 6h) between the groups.

Furthermore, we determined the mRNA expression of Ccdn1 as potential target gene of the EDA-NF-κB pathway by qPCR and found a significant reduction both in untreated and Fc-EDA-treated *Tabby* mice (Fig. 6h) compared with wild-type mice. A similar expression pattern was observed for the transcription factor Elf5 (Fig. 6h), which has an essential role during early embryogenesis and mammary gland development as well as during pregnancy and lactation [38].

Impact of Fc-EDA treatment on lactating mammary glands

Female *Tabby* mice showed abnormal lactation resulting in significantly reduced weight gain of their pups. Therefore, we also investigated the milk composition. Two key components of murine milk are ß-casein and whey acidic protein (WAP) [39]. The measurement of the respective mRNA expression revealed a significant diminishment of ß-casein mRNA and a tendency towards reduced WAP expression in mammary glands from untreated and Fc-EDA-treated *Tabby* dams at L1 (Fig. 7a). Western blot analysis using an antibody against rabbit anti-milk serum confirmed that untreated and Fc-EDA-treated protein lysates from L1 mammary glands of *Tabby* mice tend to contain less milk protein than corresponding wild-type lysates (Fig. 7b, c).

Paraffin sections of L1 mammary glands were stained with an antibody against murine milk proteins. Less milk protein was present in the acini of lactating mammary glands from *Tabby* dams compared with control animals (Fig. 7c-e). Sudan III staining of cryosections highlighted large fat droplets in the alveolar lumina of both treated and untreated *Tabby* mothers (Fig. 7f-h). The fat droplets seemed to coalesce to larger aggregates, which were not observed in wild-type glands to the same extent. Taken together, lack of functional EDA

protein leads to reduced expression of milk proteins, particularly ß-casein, in luminal cells and thus to a different milk composition which was not changed by prenatal treatment with Fc-EDA (Fig. 7a, b, d, g).

Discussion

Mikkola et al. identified a role of EDA signaling in mammary gland development [40-42]. EDA is a unique factor regulating embryonic and prepubertal mammary gland morphogenesis through activation of EDAR/NF-κB in the epithelium [7]. In the mouse model, EDA deficiency or inhibition of NF-κB led to a reduction of ductal tree size and fewer branching points [7, 43]. On the contrary, overexpression of *EDA* induced a NF-κB-dependent phenotype with amplified ductal growth and branching rates due to enhanced epithelial cell proliferation [7, 42].

Our results confirm the previously described EDA action during hormone-independent mammary gland morphogenesis. In addition, our data suggest that EDA or the stimulation of the EDA/EDAR pathway is also crucial for the hormone-dependent stages of breast development during puberty and alveologenesis/lactation. Prenatal treatment with Fc-EDA led to a significantly improved branching morphogenesis during puberty in *Tabby* mice. During lactation, untreated *Tabby* mice showed a significantly impaired breastfeeding capacity secondary to reduced mammary gland alveologenesis and nipple malformation as well as a reduced expression of milk proteins. As a result, *Tabby* pups displayed a markedly lower weight compared to age-matched wild-type pups. Our mother exchange experiments showed that the maternal EDA deficiency was causative for the reduced weight gain in the offspring. The observation that litter size affected the weight of pups also suggested that reduced availability of maternal milk was relevantly curtailing their growth. Prenatal treatment with Fc-EDA partially, yet significantly alleviated these symptoms by normalizing epithelial cell proliferation and nipple formation, thereby enabling regular weight gain of the *Tabby* offspring. However, epithelial architecture and milk composition at L1 remained unaffected.

The latter finding has to be interpreted with caution though, as the reduction in ß-casein and WAP mRNA expression could also have resulted from the limited size of the epithelial tree in *Tabby* mammary glands. Nevertheless, a functional defect in the secretory luminal epithelial cells seems plausible, since the size of the ductal tree in Fc-EDA-treated glands was almost comparable to that of wild-type glands. Noteworthy, besides the dependence on mammogenic auto-/paracrine signals [44, 45] and on epithelial-stromal/extracellular matrix interactions, mammary epithelial cell (MEC) proliferation does strongly rely on cell-cell contacts within the end bud [46]. Perturbations that disrupt end-bud integrity inhibit ductal

extension. Normal epithelial cell-cell contacts are vital for growth signal transduction (e.g. from estrogen and GH) [46]. While mammary ducts and alveoli consist of inner (luminal) epithelial cells and outer (basal) myoepithelial cells [17, 47], terminal end buds (TEBs) are composed of epithelial cap and luminal body cells. MECs are linked at their cell-cell interfaces by tight junctions, adherent junctions and desmosomes [48]. Physiologic mammary gland cell architecture is a strong prerequisite for the synthesis and secretion of milk. The zona occludens protein (ZO), one of the predominant tight junction proteins, forms a continuous band at the apical surface of the luminal epithelial cells [48]. Dislocation of ZO-1 is linked to disruption of the cell polarity protein complex and leads to a disturbed branching morphogenesis and impaired ductal barriers for cyclical changes during lactation [49, 50]. As for other molecules important for structural integrity such as E-cadherin [34], SMA [35, 37, 51] and keratin 14 (K14, [35, 36]), we did not observe a significant change in mRNA expression rate of ZO-1 in *Tabby* mice, nor were we able to identify loss of ductal/TEB integrity. However, the apical expression of ZO-1 seemed to be inhomogenously distributed among luminal epithelial cells of *Tabby* glands independent of their Fc-EDA-treatment status which might have contributed to the impaired secretory capacity of the luminal MEC in *Tabby* mammary glands. Interestingly, ZO-1 expression has been shown to be regulated by NF-κB in the epithelium of the intestine [52]. On the contrary, the epithelial distribution of occludin, an integral transmembrane tight junction protein, appeared homogenous. Thus, a potential involvement of ZO-1 in the decreased breastfeeding capacity of *Tabby* mice remains to be investigated by further functional analyses. During pregnancy the nipple increases in size both in humans and mice [28]. Similarly to mammary gland tissue, the nipples originate from embryonic ectoderm and are hence negatively affected by EDA deficiency. Both human female subjects heterozygous for an EDA mutation and female *Tabby* mice show very flat nipples with subsequent breastfeeding problems [11]. The molecular mechanisms of embryonic nipple development have been well documented in K14-PTHrP transgenic mice, where the human K14 promotor was used to drive the expression of the peptide growth factor parathyroid hormone-related protein (PTHrP). The simultaneous stimulation of PTHrP is required for the formation of a patch of nipple epidermis [53-55]. Interestingly, *PTHrP* was identified as a putative target gene of the EDA pathway [7]. Therefore it is conceivable that in the absence of EDA, PTHrP can no longer be activated by the EDA-NF-κB pathway, resulting in impaired nipple development during the embryonic stage and lactation.

Importance of the NF-κB pathway for EDA function is further suggested by our finding that *Ccdn1* expression was reduced in *Tabby* mice. As a potential target gene of the EDA-NF-κB pathway [5] and a known co-regulator of the estrogen receptor (ER) during different stages of mammary gland development [56], *Ccdn1* is a promising candidate gene for EDA-dependent regulation of various processes throughout mammary gland development, preferably during

the expansion of mammary epithelium during pregnancy. Deletion of *Ccdn1* in mice indeed leads to an arrest of mammary gland development before the lobulo-alveolar stage [57-59]. Unfortunately, intra-amniotic Fc-EDA treatment did not rescue *Ccdn1* expression in the mammary glands of *Tabby* mice, which may indicate a permanently diminished estrogen-response despite Fc-EDA treatment. Further studies are needed to clarify these findings.

During initiation of lactation and lactogenesis in particular, ductal epithelial cells undergo functional differentiation [17], mainly driven by progesterone and prolactin [60, 61] via their respective receptors [17, 62]. The exact mechanism of action of these hormones and their levels in EDA-deficient mammary glands is still unknown. In the initial phase of lactation Ccdn1 is essential for morphogenesis and side-branching of progesterone receptor(PR)-positive epithelial cells [63], while in the main phase the paracrine action of the TNF family member receptor activator of NF-κB-ligand (RANKL) seems to play an important role: Beleut et al. were able to show that ablation of RANKL in the mammary epithelium abrogated progesterone-induced morphogenesis, while its ectopic expression fully rescued the PR-deficient phenotype [63]. Similarly, systemic administration of RANKL induced mammary epithelial proliferation in the absence of progesterone signaling, and injection of a RANK signaling inhibitor interfered with progesterone-induced epithelial proliferation [63].

The fact that we did not observe significant differences in the expression of local RANKL, RANK, progesterone- and prolactin-receptors (PRLR) between groups in the study (Supplementary Fig. 1) argues against a compensatory mechanism in the absence of EDA. However, we observed a significant reduction of Elf5 expression during lactation, which might suggest an involvement of RANKL at this hormone-dependent stage of mammary gland development in *Tabby* mice. Progesterone drives mammary secretory differentiation via RANKL-mediated induction of Elf5 in luminal progenitor cells [64], making it essential for early embryogenesis and mammary gland development during pregnancy and lactation [38]. Furthermore Elf5 acts downstream of the prolactin receptor to modulate alveolar morphogenesis and secretory activity [65]. As Elf5 is a downstream target of the NF-κB pathway [43], lack of EDA and subsequently reduced NF-κB signaling might have negatively affected the local progesterone and prolactin action via Elf5 in *Tabby* mice. In line with this finding, we observed a tendency of reduced expression of PRLR in *Tabby* mice regardless of treatment, when compared to wild-type animals (Supplementary Fig. 1). Intra-amniotic administration of Fc-EDA, however, did not rescue Elf5 expression in the mammary glands of *Tabby* mice, which could argue for a permanently diminished response to the above hormones despite effective Fc-EDA treatment. This has to be addressed by future studies.

Our findings are limited by the fact that the local cross-talk of estrogen and progesterone with growth factors during day L1 remains unclear. Others have shown, however, that estrogen

receptor alpha and E2 are essential to ensure the state of terminal differentiation in mammary epithelial cells [66] while progesterone receptor isoforms were undetectable in ducts and alveoli at day L10 in mice [67]. Furthermore, our gene expression analysis was based on total RNA extracted from mammary gland whole mounts. Therefore, the ratio of epithelium to stroma might have varied. Although epithelial and stromal housekeeping genes were chosen, future studies with epithelial extracts might be necessary to verify our results. We also did not run functional tests to assess tight junction patency, such as analyses of milk composition. It thus remains to be clarified, whether a disorganization of ZO-1 may have contributed to the impaired breastfeeding behavior of *Tabby* mice.

Taken together, EDA seems to play roles in embryonic and prepubertal mammary gland development [7], but possibly also in post-developmental mammary gland physiology. Administration of recombinant EDA during murine embryogenesis has a considerable impact on mammary gland morphogenesis. Remarkably, this translates into the improvement of several features that develop subsequently, when the recombinant protein is most probably no longer present: nipple formation, alveologenesis, and mammary epithelial function during puberty and lactation. Our study shows that activation of the EDAR pathway during embryonic development of *Tabby* fetuses improves, but does not fully correct, the mammary gland phenotype that is observed when the treated fetuses have reached adulthood. Whether recombinant EDA cannot fully recapitulate the action of native endogenous EDA, or whether the EDA-EDAR pathway is activated again after embryonic development, e.g. at puberty or during pregnancy, will be interesting to investigate in the future. Some of our observations have already been confirmed in human HED patients who show similar disorders of breast development as *Tabby* mice [11]. For the affected women, this is of major psychological relevance during puberty, adolescence, and especially when breastfeeding.

Conflict of Interest

P.S. is a shareholder of Edimer Pharmaceuticals. P.S. and H.S. hold patents relevant to this publication. The other authors declare that they have no conflict of interest.

Figure captions

Fig. 1: *Growth restriction of newborn Tabby mice depends on the mother*
(a) Weight gain of pups in 32 wild-type (wt) and 24 *Tabby* litters was recorded daily from birth to weaning. The dotted line at P17 indicates the time point used for the analyses shown in panels b-e. **(b)** Weight of native *Tabby* and wt pups at P17. **(c)** Weight of *Tabby* (black bars) or wt (striped bars) pups at P17, as a function of litter size. Animal numbers analyzed per condition are indicated. Conditions with 4 pups/litter were compared statistically to those of smaller or larger litters. **(d)** Weights of male and female *Tabby* (black bars) or wt (striped bars) pups in litters of 5 to 7 animals. **(e)** Comparison of the weight of *Tabby* (Tb) or wt pups left with their mothers or transferred at P1 to foster mothers. Black bar: wt pups with Tb dams. Grey bar: Tb pups with Tb dams. White striped bar: wt pups with wt dams. Grey striped bar: Tb pups with Tb dams. Data are shown as mean ± SD; P-values: ns (p>0.05); **(p<0.01); ***(p<0.001).

Fig. 2: *Nipple development following prenatal treatment with Fc-EDA*
(a-c) Macroscopic comparison of representative nipples from untreated *Tabby* **(a)** Fc-EDA-treated *Tabby* **(b)** and wild-type **(c)** female mice on day 1 of lactation (L1). **(d)** Semi-quantitative assessment of the nipple morphology. 1, flat; 2, cubical; 3, cylindrical. Untreated nipple score (n=7): 1.57±0.2; Fc-EDA-treated *Tabby* (n=4)*:* 2.5±0.29; wild-type nipple (n=11): 2.6±0.15. Data are shown as mean ± SEM; P-values: *(<0.05); **(p<0.01).

Fig. 3: *Impact of prenatal treatment on breastfeeding efficacy*
(a) Body weight development of pups from untreated *Tabby*, Fc-EDA-treated *Tabby* and wild-type mothers. **(b)** Body mass index (body weight/body length²) of 10-day-old pups from untreated *Tabby*, Fc-EDA-treated *Tabby* and wild-type mothers. **(c)** Weight differences between untreated *Tabby* (black bars), Fc-EDA-treated *Tabby* (white bars) and wild-type pups (striped bars) at P17 were sex-independent. Data are shown as mean ± SEM; P-values: **(p<0.01); ***(p<0.001), ****(p<0.0001).

Fig. 4: *Mammary gland whole mount analysis of branching morphogenesis*
(a-f) Carmine-stained whole mounts of representative mammary glands from untreated *Tabby* (a,d), Fc-EDA-treated *Tabby* (b, e) and wild-type (wt) mice (c, f) at day P42 (Scale bar: a-c: 500 µm; d-f: 1 mm) **(d-f)** In panels d-f, the outer limits of the gland (black dotted line)

and the ductal tree (blue lines) are shown. **(g)** Quantification of end tips as sum of end tips and end buds. **(h)** Comparison of branch point numbers in the three groups. A significantly improved structural development of mammary glands was observed in Fc-EDA-treated *Tabby* (white bars) versus *Tabby* (black bars) female mice at the pre-pubertal stage and during puberty (P21 and P42, respectively), which was comparable with that of wild-type controls (grey bars). **(i)** Ductal outgrowth was quantified as percentage of fat pad filled by ducts, using the ratio of areas delimited by blue and black dotted lines in panels d-f. Data are shown as mean ± SEM; P-values: *($p<0.05$); **($p=0.001-0.01$); ***($p<0.001$).

Fig. 5: *Effects of prenatal treatment with Fc-EDA on alveologenesis*

(a-c) Carmine-stained whole mounts of representative untreated *Tabby*, Fc-EDA-treated *Tabby* and wild-type mammary glands on day L1. **(d-f, d`-f`)** Hematoxylin-eosin-stained sections of mammary glands from untreated *Tabby*, Fc-EDA-treated *Tabby* and wild-type (wt) on day L1, indicating different alveolar densities. **(d`-f`)** represent higher magnifications of the samples shown in panel d-f. **(d`, e`)** Cytoplasmic lipid droplets in *Tabby* mammary glands are marked by white arrow heads. **(g-i)** Representative immunofluorescence staining for PCNA (red) on day L1. **(j)** Quantification of the alveolar density prior to gestation (n.l.), on days 14.5 and 18.5 of gestation and at L1. **(k)** Quantification of PCNA-positive nuclei of glands from untreated *Tabby*, Fc-EDA-treated *Tabby* and wild-type mice at days P42 and L1. **(l)** Quantification of TUNEL-positive cells at days P42 and L1. Scale bar in d: 100 µm. Scale bar in d`: 50 µm. Data are shown as mean ± SEM; P-values: **($p=0.001-0.01$); ***($p<0.001$); not significant ($p>0.05$).

Fig. 6: *Epithelial cell architecture and expression of NF-κB downstream targets during lactation*

(a-c) Immunostaining for the apical cell marker ZO-1 (red) and the cytoskeleton marker E-cadherin (E-cad, green). Magnified pictures beneath, where the two fluorescent channels are shown separately as well as merged, indicate irregular deposition of ZO-1 in *Tabby* mice (white arrowheads in a, b). **(d-f)** Immunostaining for Keratin 14 (K14, red) and the basal cell marker smooth muscle actin (SMA, green). **(a-f)** Cell nuclei were stained blue with DAPI. **(g, h)** Relative gene expression (quantitative RT-PCR) of the epithelial cell markers stained in a-f, as well as Ccdn1, Elf5 and EDA in untreated *Tabby* (black bars), Fc-EDA-treated *Tabby* (white bars) and wild-type (striped bars) mammary gland tissue at day L1. Scale bars in a-d: 50 µm. Data are shown as mean ± SEM; P-values: **(g)** not significant ($p>0.05$); **(h)** *($p<0.05$); ***($p<0.001$); ****($p<0.0001$).

Fig. 7: *No therapeutic effects on epithelial function in the lactating mammary gland*

(a) Relative gene expression of the two milk proteins β-casein and whey acidic protein (WAP) in untreated *Tabby* (black bars), Fc-EDA-treated *Tabby* (white bars) and wild-type mothers' (striped bars) L1 mammary gland tissue, as measured by quantitative RT-PCR. **(b)** Western blot of milk proteins from mammary gland tissue at L1 (inguinal glands from three different females per group). Each lane represents an individual gland from one animal. Non-lactating (n.l.) mammary glands from adult wild-type female mice were used as control tissue. GAPDH served as loading control. **(c)** Optical densitometric estimation of Casein protein level normalized to GAPDH. **(d-f)** Immunostaining of murine milk proteins in the acini of mammary glands at L1 (Scale bar: 50 µm). **(g-i)** Sudan III staining of cryosections at L1 revealed large fat droplets in the lumina of alveoli from both untreated and Fc-EDA-treated *Tabby* mice (Scale bar: 100 µm). Data are shown as mean ±SEM; P-values: ns($p > 0.05$); *($p < 0.05$); **($p = 0.001 - 0.01$); ***($p < 0.001$).

Supplement

Supplementary Fig. 1: *Hormone-related alterations in Tabby mammary glands.*

Relative gene expression of RANKL, its receptor RANK, and the hormone receptors for progesterone (PGR), estrogen (ESR1) and prolactin (PRLR) in *Tabby* (black bars), Fc-EDA-treated *Tabby* (white bars) and wild-type (striped bars) mammary gland tissue at day L1, as measured by quantitative RT-PCR. Data are shown as mean ± SEM; P-values: not significant ($p > 0.05$).

Supplementary Fig. 2: *Nipple morphology scores.*

Representative example of **(a)** flat (score 1) **(b)** cubical (score 2) and **(c)** cylindrical nipples (score 3) of female mice on day 1 of lactation (L1).

Supplementary Fig. S3: *Epithelial tight junction barrier.*

(a-c) Immunostaining for the tight junction protein occludin (red) in mammary glands from untreated *Tabby*, Fc-EDA-treated *Tabby* and wild-type mice on day L1. Cell nuclei were stained blue with DAPI. The scale bar in a-c represents 50 µm.

References

1. Clarke A. Hypohidrotic ectodermal dysplasia. J Med Genet. 1987;24(11):659-63.
2. Visinoni AF, Lisboa-Costa T, Pagnan NA, Chautard-Freire-Maia EA. Ectodermal dysplasias: clinical and molecular review. Am J Med Genet A. 2009;149a(9):1980-2002.
3. Cluzeau C, Hadj-Rabia S, Jambou M, Mansour S, Guigue P, Masmoudi S et al. Only four genes (EDA1, EDAR, EDARADD, and WNT10A) account for 90% of hypohidrotic/anhidrotic ectodermal dysplasia cases. Hum Mutat. 2011;32(1):70-2.
4. Kowalczyk-Quintas C, Schneider P. Ectodysplasin A (EDA) - EDA receptor signalling and its pharmacological modulation. Cytokine Growth Factor Rev. 2014;25(2):195-203.
5. Schmidt-Ullrich R, Tobin DJ, Lenhard D, Schneider P, Paus R, Scheidereit C. NF-kappaB transmits Eda A1/EdaR signalling to activate Shh and cyclin D1 expression, and controls post-initiation hair placode down growth. Development. 2006;133(6):1045-57.
6. Fliniaux I, Mikkola ML, Lefebvre S, Thesleff I. Identification of dkk4 as a target of Eda-A1/Edar pathway reveals an unexpected role of ectodysplasin as inhibitor of Wnt signalling in ectodermal placodes. Dev Biol. 2008;320(1):60-71.
7. Voutilainen M, Lindfors PH, Lefebvre S, Ahtiainen L, Fliniaux I, Rysti E et al. Ectodysplasin regulates hormone-independent mammary ductal morphogenesis via NF-kappaB. Proc Natl Acad Sci USA. 2012;109(15):5744-9.
8. Kere J, Srivastava AK, Montonen O, Zonana J, Thomas N, Ferguson B et al. X-linked anhidrotic (hypohidrotic) ectodermal dysplasia is caused by mutation in a novel transmembrane protein. Nat Genet. 1996;13(4):409-16.
9. Headon DJ, Emmal SA, Ferguson BM, Tucker AS, Justice MJ, Sharpe PT et al. Gene defect in ectodermal dysplasia implicates a death domain adapter in development. Nature. 2001;414(6866):913-6.
10. Monreal AW, Ferguson BM, Headon DJ, Street SL, Overbeek PA, Zonana J. Mutations in the human homologue of mouse dl cause autosomal recessive and dominant hypohidrotic ectodermal dysplasia. Nat Genet. 1999;22(4):366-9.
11. Wahlbuhl-Becker M, Faschingbauer F, Beckmann MW, Schneider H. Hypohidrotic Ectodermal Dysplasia: Breastfeeding Complications Due to Impaired Breast Development. Geburtshilfe Frauenheilkd. 2017;77(4):377-382.
12. Heckmann U. Congenital bilateral amastia in a mother and a daughter Geburtshilfe Frauenheilkd. 1982;42(4):318-20.
13. Al Marzouqi F, Michot C, Dos Santos S, Bonnefont JP, Bodemer C, Hadj-Rabia S. Bilateral amastia in a female with X-linked hypohidrotic ectodermal dysplasia. Br J Dermatol. 2014;171(3):671-3.
14. Wohlfart S, Soder S, Smahi A, Schneider H. A novel missense mutation in the gene EDARADD associated with an unusual phenotype of hypohidrotic ectodermal dysplasia. Am J Med Genet A. 2016;170a(1):249-53.
15. Haghighi A, Nikuei P, Haghighi-Kakhki H, Saleh-Gohari N, Baghestani S, Krawitz PM et al. Whole-exome sequencing identifies a novel missense mutation in EDAR causing autosomal recessive hypohidrotic ectodermal dysplasia with bilateral amastia and palmoplantar hyperkeratosis. Br J Dermatol. 2013;168(6):1353-6.
16. Megarbane H, Cluzeau C, Bodemer C, Fraitag S, Chababi-Atallah M, Megarbane A et al. Unusual presentation of a severe autosomal recessive anhydrotic ectodermal dysplasia with a novel mutation in the EDAR gene. Am J Med Genet A. 2008;146a(20):2657-62.
17. Hennighausen L, Robinson GW. Information networks in the mammary gland. Nat Rev Mol Cell Biol. 2005;6(9):715-25.
18. Falconer DS. A totally sex-linked gene in the house mouse. Nature. 1952;169(4303):664-5.

19. Srivastava AK, Montonen O, Saarialho-Kere U, Chen E, Baybayan P, Pispa J et al. Fine mapping of the EDA gene: a translocation breakpoint is associated with a CpG island that is transcribed. Am J Hum Genet. 1996;58(1):126-32.

20. Srivastava AK, Pispa J, Hartung AJ, Du Y, Ezer S, Jenks T et al. The Tabby phenotype is caused by mutation in a mouse homologue of the EDA gene that reveals novel mouse and human exons and encodes a protein (ectodysplasin-A) with collagenous domains. Proc Natl Acad Sci USA. 1997;94(24):13069-74.

21. Gaide O, Schneider P. Permanent correction of an inherited ectodermal dysplasia with recombinant EDA. Nat Med. 2003;9(5):614-8.

22. Hermes K, Schneider P, Krieg P, Dang A, Huttner K, Schneider H. Prenatal therapy in developmental disorders: drug targeting via intra-amniotic injection to treat X-linked hypohidrotic ectodermal dysplasia. J Invest Dermatol. 2014;134(12):2985-7.

23. Dunphy KA, Tao L, Jerry DJ. Mammary epithelial transplant procedure. J Vis Exp. 2010;(40).

24. Schindelin J, Rueden CT, Hiner MC, Eliceiri KW. The ImageJ ecosystem: An open platform for biomedical image analysis. Mol Reprod Dev. 2015;82(7-8):518-29.

25. Beinder L, Faehrmann N, Wachtveitl R, Winterfeld I, Hartner A, Menendez-Castro C et al. Detection of expressional changes induced by intrauterine growth restriction in the developing rat mammary gland via exploratory pathways analysis. PLoS One. 2014;9(6):e100504.

26. Podzus J, Kowalczyk-Quintas C, Schuepbach-Mallepell S, Willen L, Staehlin G, Vigolo M et al. Ectodysplasin A in Biological Fluids and Diagnosis of Ectodermal Dysplasia. J Dent Res. 2017;96(2):217-224.

27. Blecher SR. Anhidrosis and absence of sweat glands in mice hemizygous for the Tabby gene: supportive evidence for the hypothesis of homology between Tabby and human anhidrotic (hypohidrotic) ectodermal dysplasia (Christ-Siemens-Touraine syndrome). J Invest Dermatol. 1986;87(6):720-2.

28. Toyoshima Y, Ohsako S, Nagano R, Matsumoto M, Hidaka S, Nishinakagawa H. Histological changes in mouse nipple tissue during the reproductive cycle. J Vet Med Sci. 1998;60(4):405-11.

29. Affolter M, Bellusci S, Itoh N, Shilo B, Thiery JP, Werb Z. Tube or not tube: remodeling epithelial tissues by branching morphogenesis. Dev Cell. 2003;4(1):11-8.

30. Oakes SR, Hilton HN, Ormandy CJ. The alveolar switch: coordinating the proliferative cues and cell fate decisions that drive the formation of lobuloalveoli from ductal epithelium. Breast Cancer Res. 2006;8(2):207.

31. Palmer CA, Neville MC, Anderson SM, Mcmanaman JL. Analysis of lactation defects in transgenic mice. J Mammary Gland Biol Neoplasia. 2006;11(3-4):269-82.

32. Schwertfeger KL, Mcmanaman JL, Palmer CA, Neville MC, Anderson SM. Expression of constitutively activated Akt in the mammary gland leads to excess lipid synthesis during pregnancy and lactation. J Lipid Res. 2003;44(6):1100-12.

33. Paine IS, Lewis MT. The Terminal End Bud: the Little Engine that Could. J Mammary Gland Biol Neoplasia. 2017.

34. Boussadia O, Kutsch S, Hierholzer A, Delmas V, Kemler R. E-cadherin is a survival factor for the lactating mouse mammary gland. Mech Dev. 2002;115(1-2):53-62.

35. Mikaelian I, Hovick M, Silva KA, Burzenski LM, Shultz LD, Ackert-Bicknell CL et al. Expression of terminal differentiation proteins defines stages of mouse mammary gland development. Vet Pathol. 2006;43(1):36-49.

36. Sun P, Yuan Y, Li A, Li B, Dai X. Cytokeratin expression during mouse embryonic and early postnatal mammary gland development. Histochem Cell Biol. 2010;133(2):213-21.

37. Deugnier MA, Moiseyeva EP, Thiery JP, Glukhova M. Myoepithelial cell differentiation in the developing mammary gland: progressive acquisition of smooth muscle phenotype. Dev Dyn. 1995;204(2):107-17.

38. Zhou J, Chehab R, Tkalcevic J, Naylor MJ, Harris J, Wilson TJ et al. Elf5 is essential for early embryogenesis and mammary gland development during pregnancy and lactation. Embo j. 2005;24(3):635-44.

39. Hennighausen L, Westphal C, Sankaran LPittius CW. Regulation of expression of genes for milk proteins. Biotechnology. 1991;16:65-74.
40. Lindfors PH, Voutilainen M, Mikkola ML. Ectodysplasin/NF-kappaB signaling in embryonic mammary gland development. J Mammary Gland Biol Neoplasia. 2013;18(2):165-9.
41. Mikkola ML. TNF superfamily in skin appendage development. Cytokine Growth Factor Rev. 2008;19(3-4):219-30.
42. Mustonen T, Pispa J, Mikkola ML, Pummila M, Kangas AT, Pakkasjarvi L et al. Stimulation of ectodermal organ development by Ectodysplasin-A1. Dev Biol. 2003;259(1):123-36.
43. Barham W, Chen L, Tikhomirov O, Onishko H, Gleaves L, Stricker TP et al. Aberrant activation of NF-kappaB signaling in mammary epithelium leads to abnormal growth and ductal carcinoma in situ. BMC Cancer. 2015;15:647.
44. Mikkola ML, Millar SE. The mammary bud as a skin appendage: unique and shared aspects of development. J Mammary Gland Biol Neoplasia. 2006;11(3-4):187-203.
45. Veltmaat JM, Mailleux AA, Thiery JP, Bellusci S. Mouse embryonic mammogenesis as a model for the molecular regulation of pattern formation. Differentiation. 2003;71(1):1-17.
46. Hinck L, Silberstein GB. Key stages in mammary gland development: the mammary end bud as a motile organ. Breast Cancer Res. 2005;7(6):245-51.
47. Inman JL, Robertson C, Mott JD, Bissell MJ. Mammary gland development: cell fate specification, stem cells and the microenvironment. Development. 2015;142(6):1028-42.
48. Owens MB, Hill AD, Hopkins AM. Ductal barriers in mammary epithelium. Tissue Barriers. 2013;1(4):e25933.
49. Nagaoka K, Udagawa T, Richter JD. CPEB-mediated ZO-1 mRNA localization is required for epithelial tight-junction assembly and cell polarity. Nat Commun. 2012;3:675.
50. Hurd TW, Gao L, Roh MH, Macara IG, Margolis B. Direct interaction of two polarity complexes implicated in epithelial tight junction assembly. Nat Cell Biol. 2003;5(2):137-42.
51. Adriance MC, Inman JL, Petersen OW, Bissell MJ. Myoepithelial cells: good fences make good neighbors. Breast Cancer Res. 2005;7(5):190-7.
52. Ma TY, Iwamoto GK, Hoa NT, Akotia V, Pedram A, Boivin MA et al. TNF-alpha-induced increase in intestinal epithelial tight junction permeability requires NF-kappa B activation. Am J Physiol Gastrointest Liver Physiol. 2004;286(3):G367-76.
53. Abdalkhani A, Sellers R, Gent J, Wulitich H, Childress S, Stein B et al. Nipple connective tissue and its development: insights from the K14-PTHrP mouse. Mech Dev. 2002;115(1-2):63-77.
54. Foley J, Dann P, Hong J, Cosgrove J, Dreyer B, Rimm D et al. Parathyroid hormone-related protein maintains mammary epithelial fate and triggers nipple skin differentiation during embryonic breast development. Development. 2001;128(4):513-25.
55. Wysolmerski JJ, Philbrick WM, Dunbar ME, Lanske B, Kronenberg H, Broadus AE. Rescue of the parathyroid hormone-related protein knockout mouse demonstrates that parathyroid hormone-related protein is essential for mammary gland development. Development. 1998;125(7):1285-94.
56. Manavathi B, Samanthapudi VS, Gajulapalli VN. Estrogen receptor coregulators and pioneer factors: the orchestrators of mammary gland cell fate and development. Front Cell Dev Biol. 2014;2:34.
57. Fantl V, Edwards PA, Steel JH, Vonderhaar BK, Dickson C. Impaired mammary gland development in Cyl-1(-/-) mice during pregnancy and lactation is epithelial cell autonomous. Dev Biol. 1999;212(1):1-11.
58. Fantl V, Stamp G, Andrews A, Rosewell I, Dickson C. Mice lacking cyclin D1 are small and show defects in eye and mammary gland development. Genes Dev. 1995;9(19):2364-72.

59. Sicinski P, Donaher JL, Parker SB, Li T, Fazeli A, Gardner H et al. Cyclin D1 provides a link between development and oncogenesis in the retina and breast. Cell. 1995;82(4):621-30.

60. Cordero A, Pellegrini P, Sanz-Moreno A, Trinidad EM, Serra-Musach J, Deshpande C et al. RankL impairs lactogenic differentiation through inhibition of the Prolactin/Stat5 Pathway at midgestation. Stem Cells. 2016;34(4):1027-39.

61. Sternlicht MD, Kouros-Mehr H, Lu P, Werb Z. Hormonal and local control of mammary branching morphogenesis. Differentiation. 2006;74(7):365-81.

62. Zeps N, Bentel JM, Papadimitriou JM, Dawkins HJ. Murine progesterone receptor expression in proliferating mammary epithelial cells during normal pubertal development and adult estrous cycle. Association with eralpha and erbeta status. J Histochem Cytochem. 1999;47(10):1323-30.

63. Beleut M, Rajaram RD, Caikovski M, Ayyanan A, Germano D, Choi Y et al. Two distinct mechanisms underlie progesterone-induced proliferation in the mammary gland. Proc Natl Acad Sci USA. 2010;107(7):2989-94.

64. Lee HJ, Gallego-Ortega D, Ledger A, Schramek D, Joshi P, Szwarc MM et al. Progesterone drives mammary secretory differentiation via RankL-mediated induction of Elf5 in luminal progenitor cells. Development. 2013;140(7):1397-401.

65. Oakes SR, Rogers RL, Naylor MJ, Ormandy CJ. Prolactin regulation of mammary gland development. J Mammary Gland Biol Neoplasia. 2008;13(1):13-28.

66. Shyamala G, Chou YC, Louie SG, Guzman RC, Smith GH, Nandi S. Cellular expression of estrogen and progesterone receptors in mammary glands: regulation by hormones, development and aging. J Steroid Biochem Mol Biol. 2002;80(2):137-48.

67. Aupperlee MD, Smith KT, Kariagina A, Haslam SZ. Progesterone receptor isoforms A and B: temporal and spatial differences in expression during murine mammary gland development. Endocrinology. 2005;146(8):3577-88.
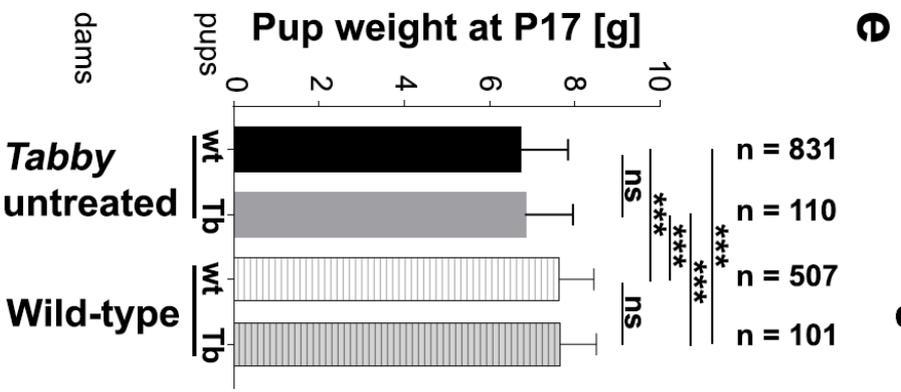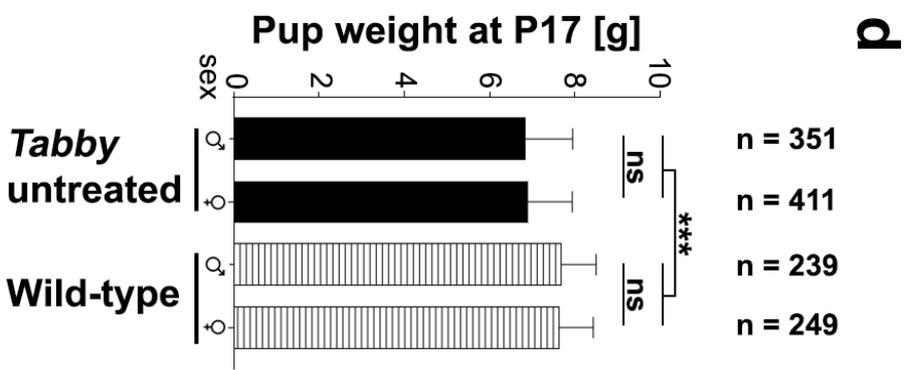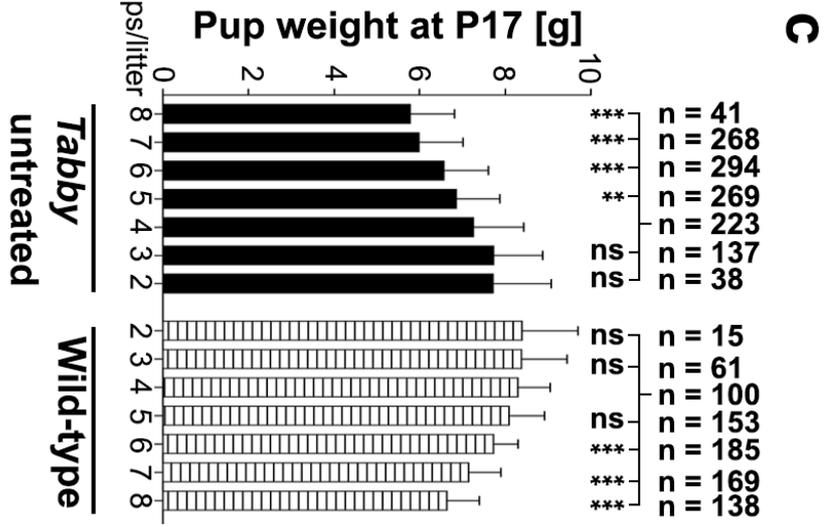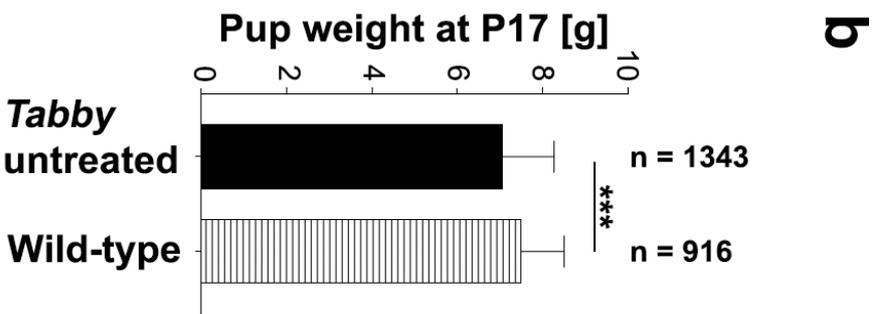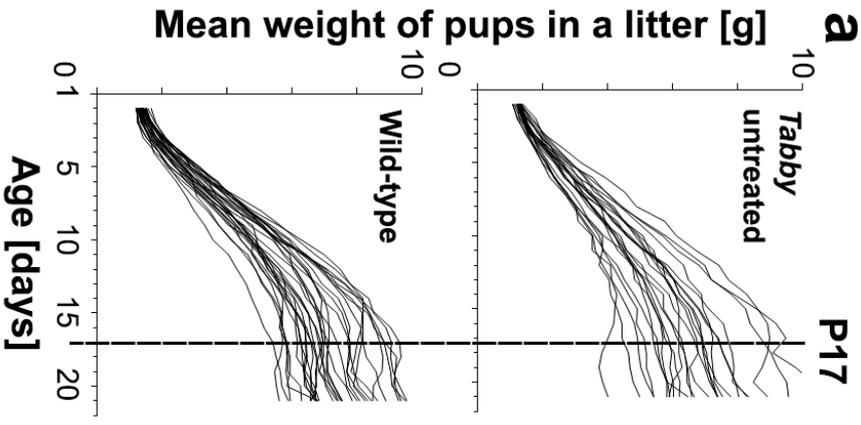
Fig. 1
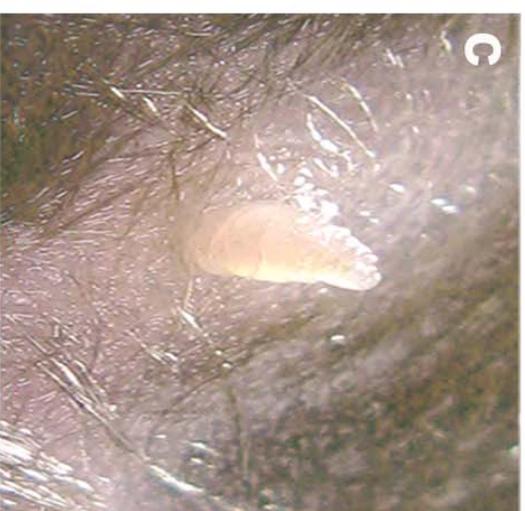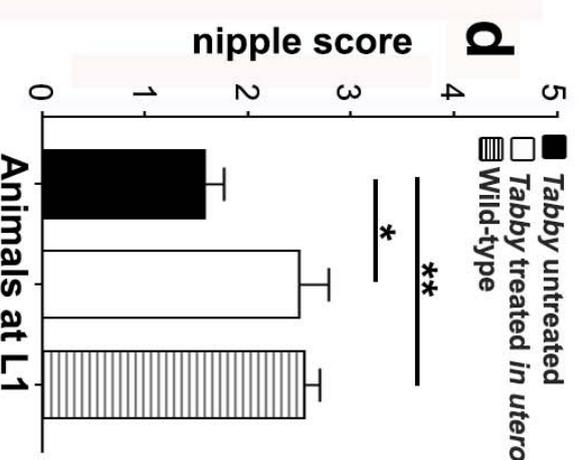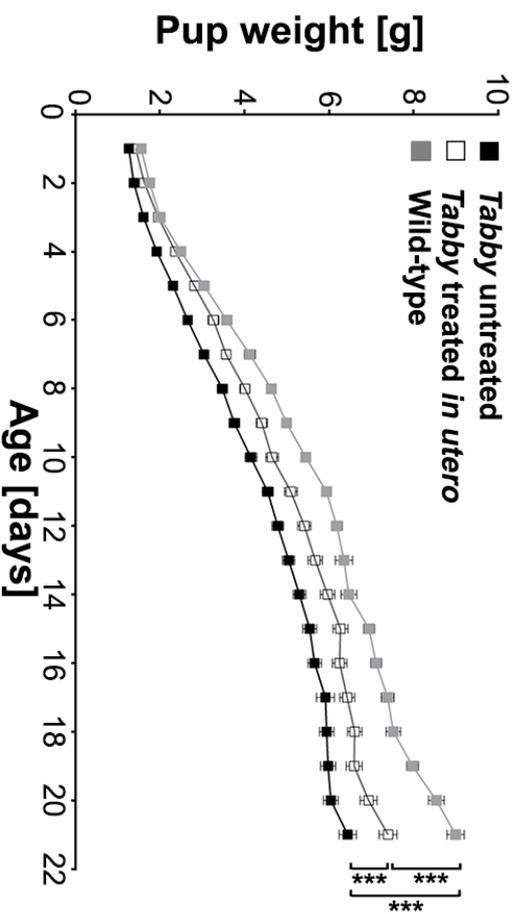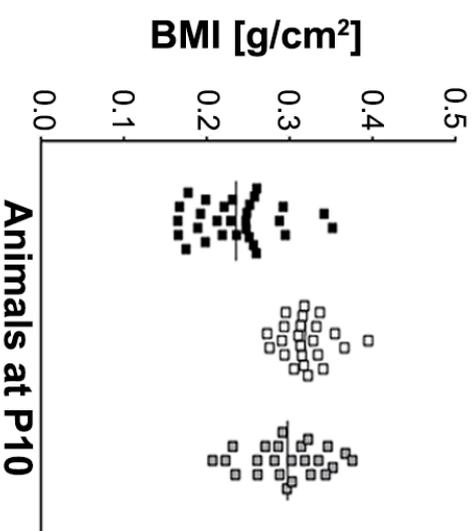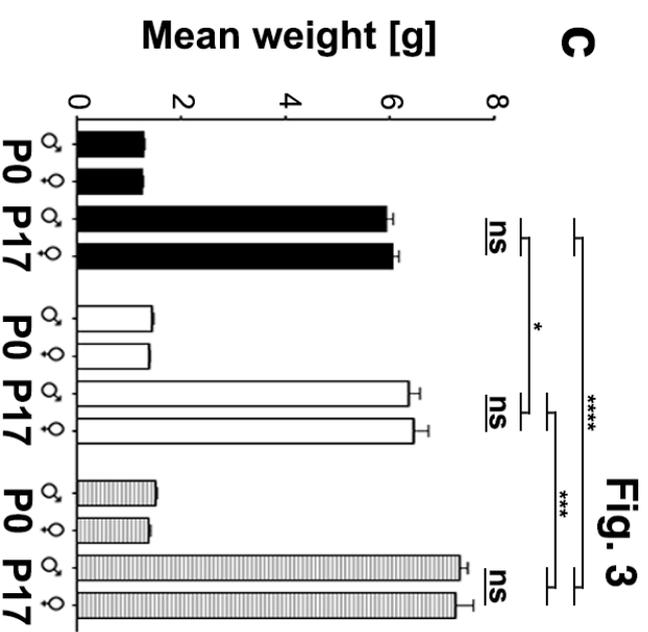
a *Tabby* untreated

b *Tabby* treated *in utero*

c Wild-type

d

nipple score

0 1 2 3 4 5

■ *Tabby* untreated
□ *Tabby* treated *in utero*
▥ Wild-type

Animals at L1

*

**

Fig. 2

Fig. 3

Fig. 4

Fig.5

Fig. 6

a *Tabby untreated*   **b** *Tabby treated in utero*   **c** Wild-type

DAPI/ZO-1/E-cad

d   **e**   **f**

DAPI/K14/SMA

g

Relative fold change

E-cad   K14   SMA   ZO-1

■ Tabby untreated
□ Tabby treated in utero
▥ Wild-type

h

Relative fold change

Ccdn1   Elf5   EDA

****
***
*
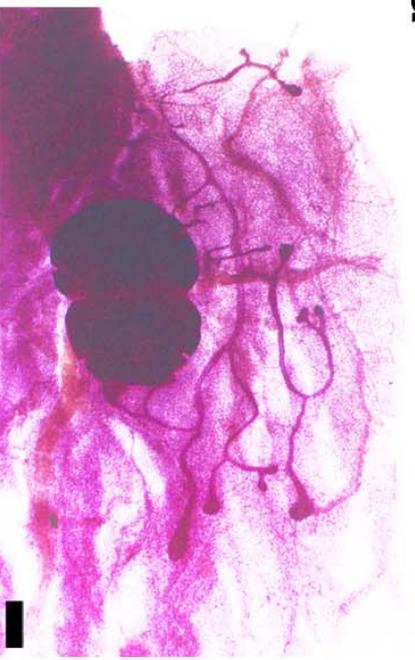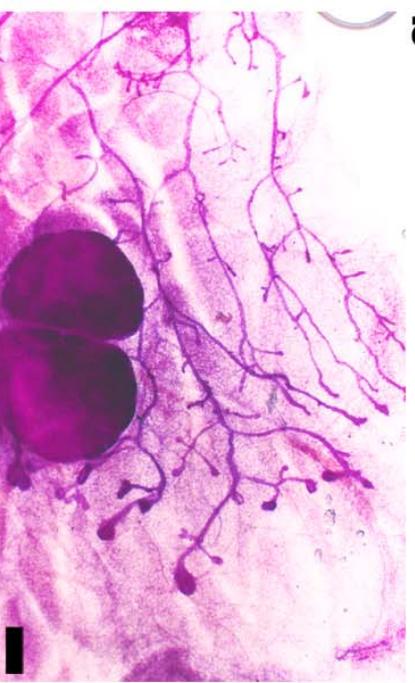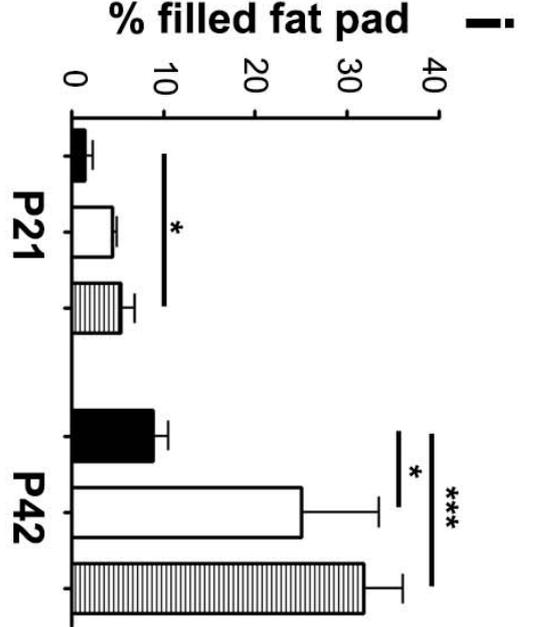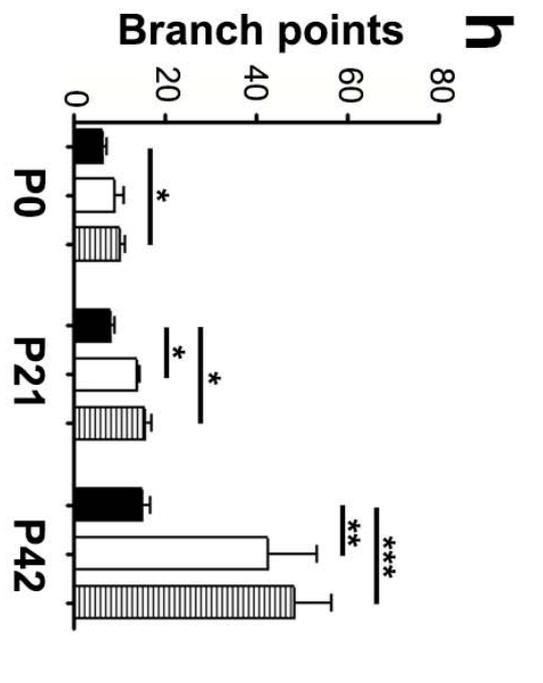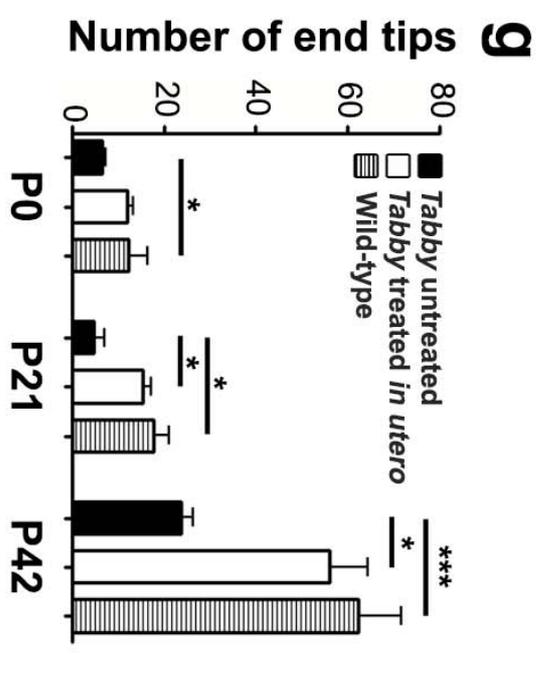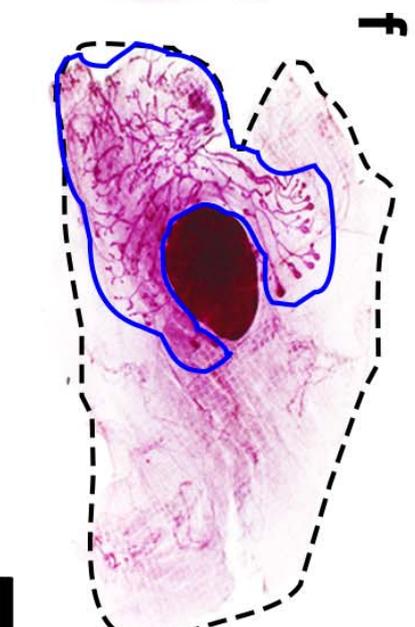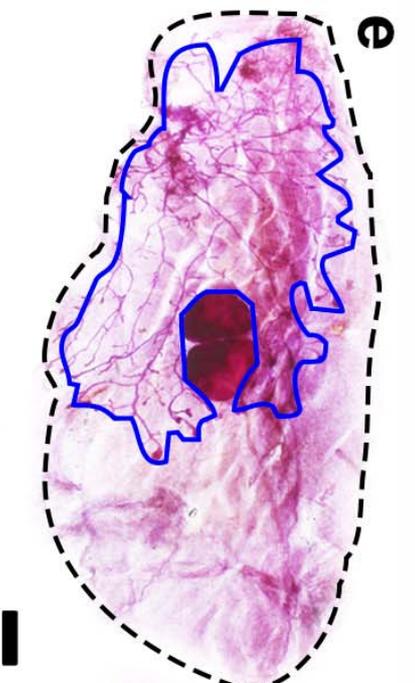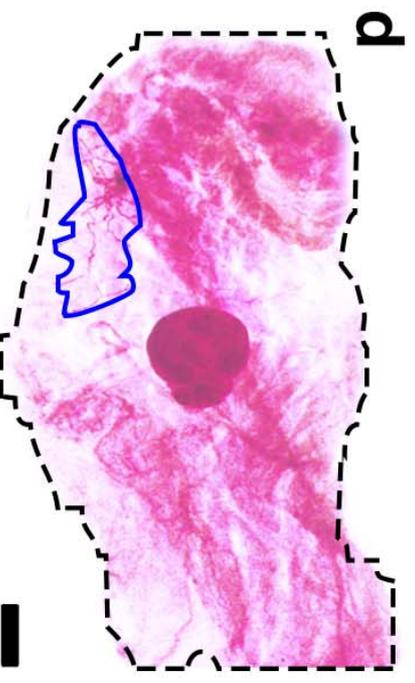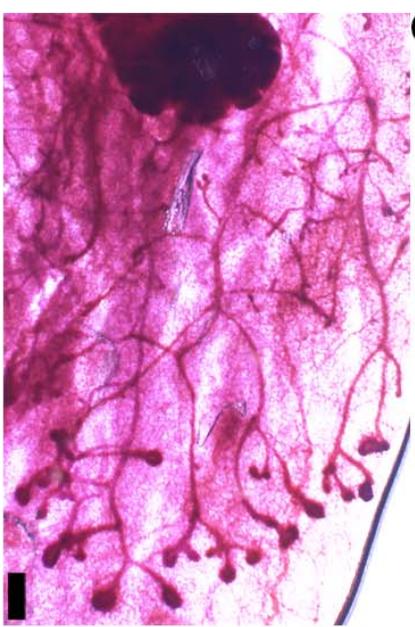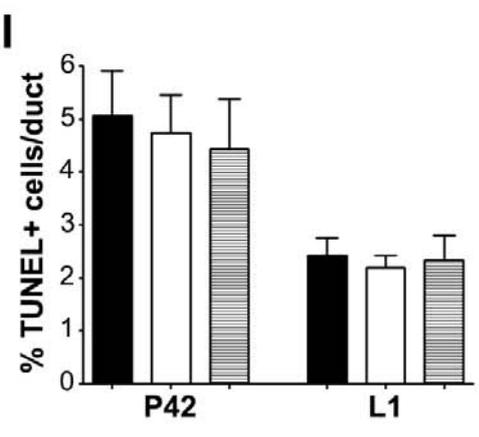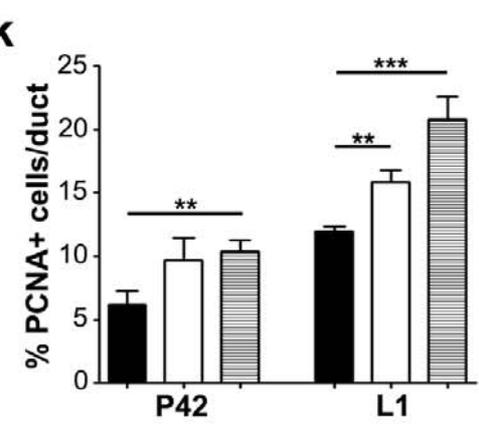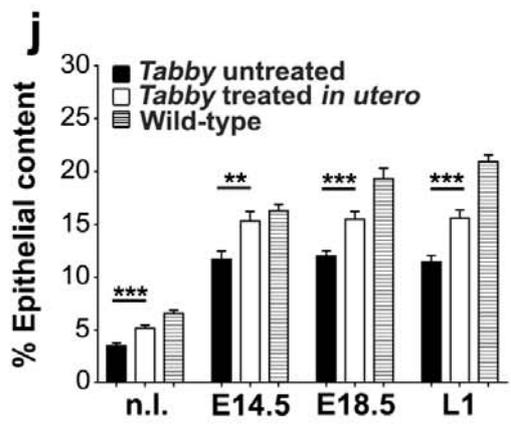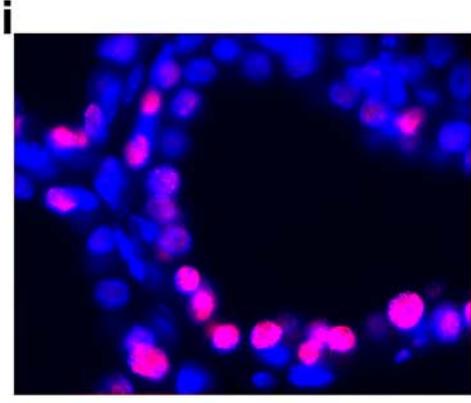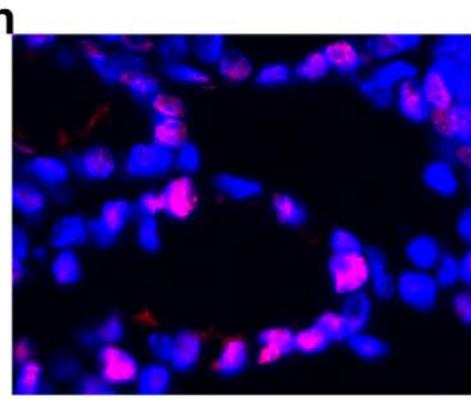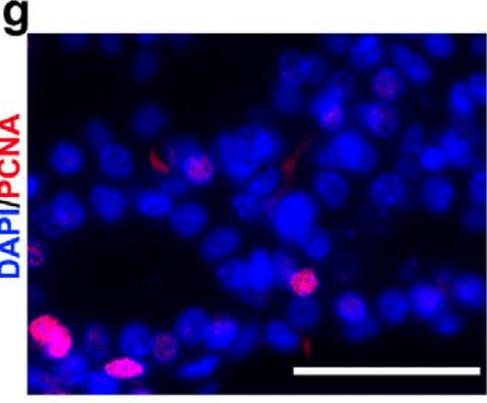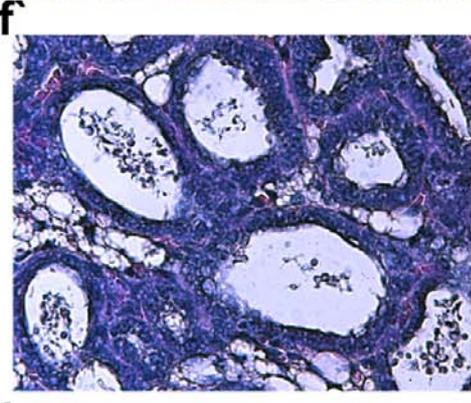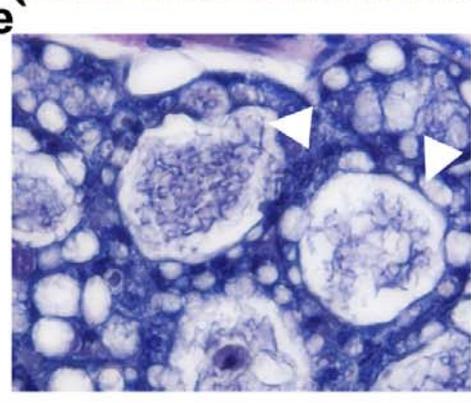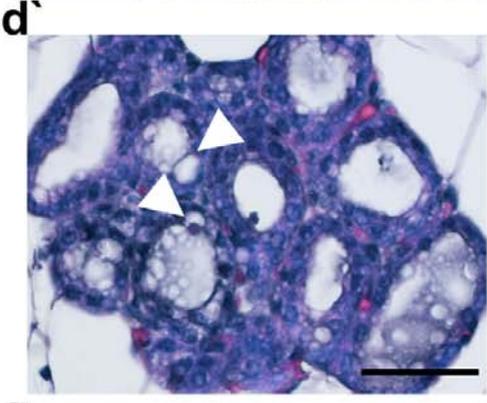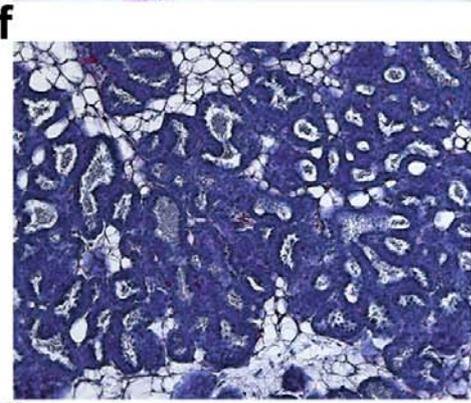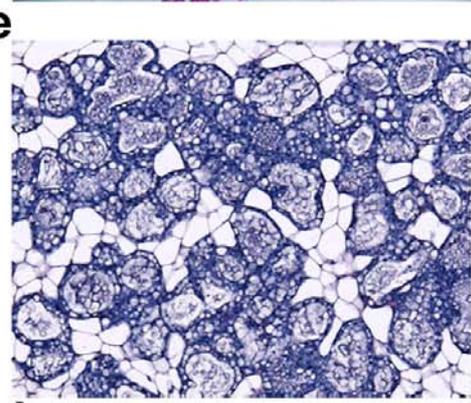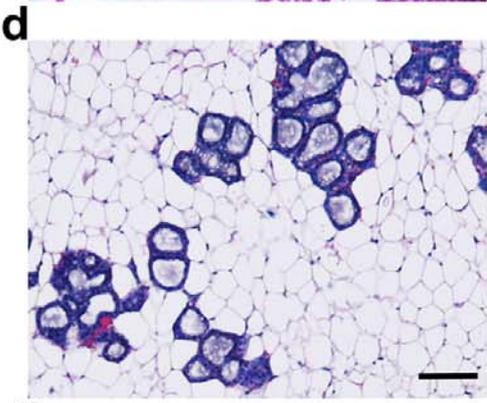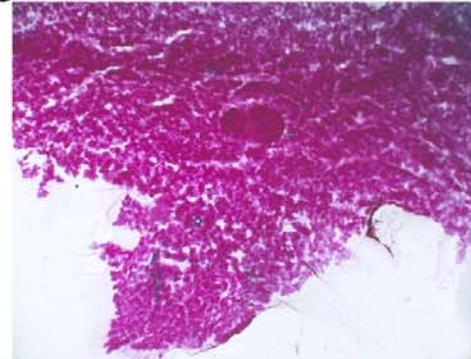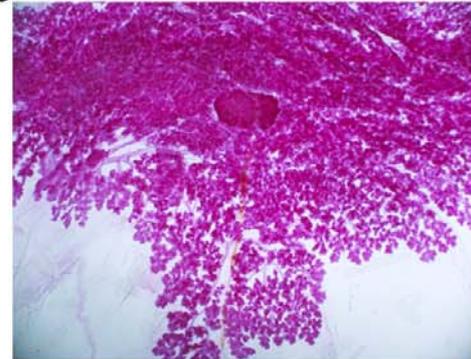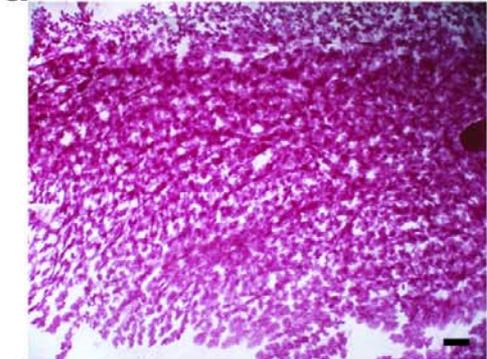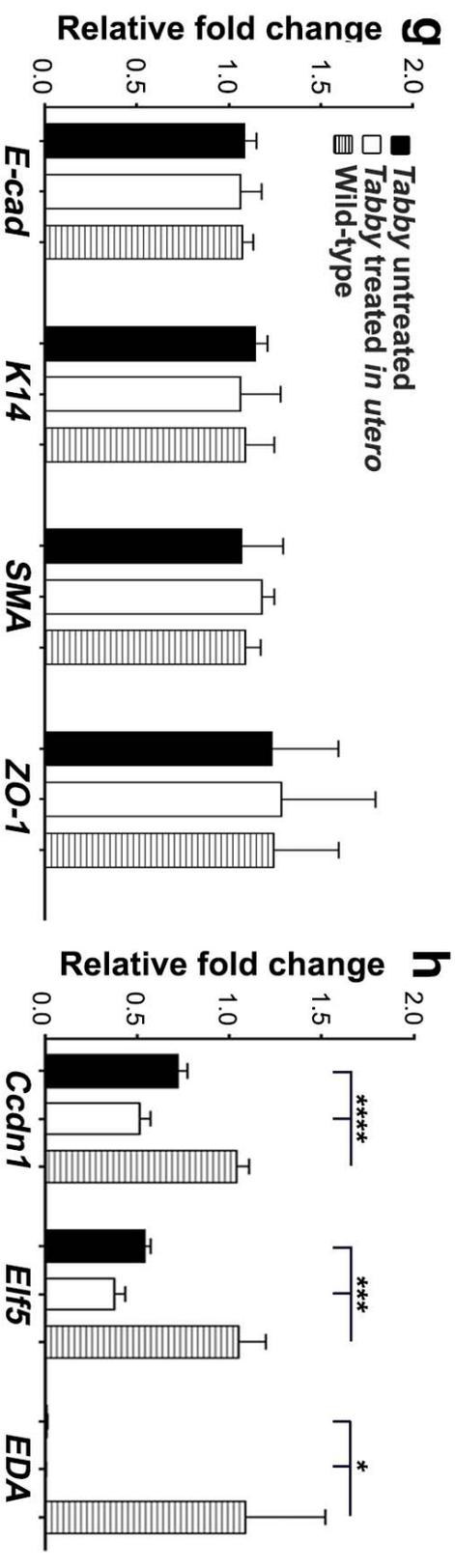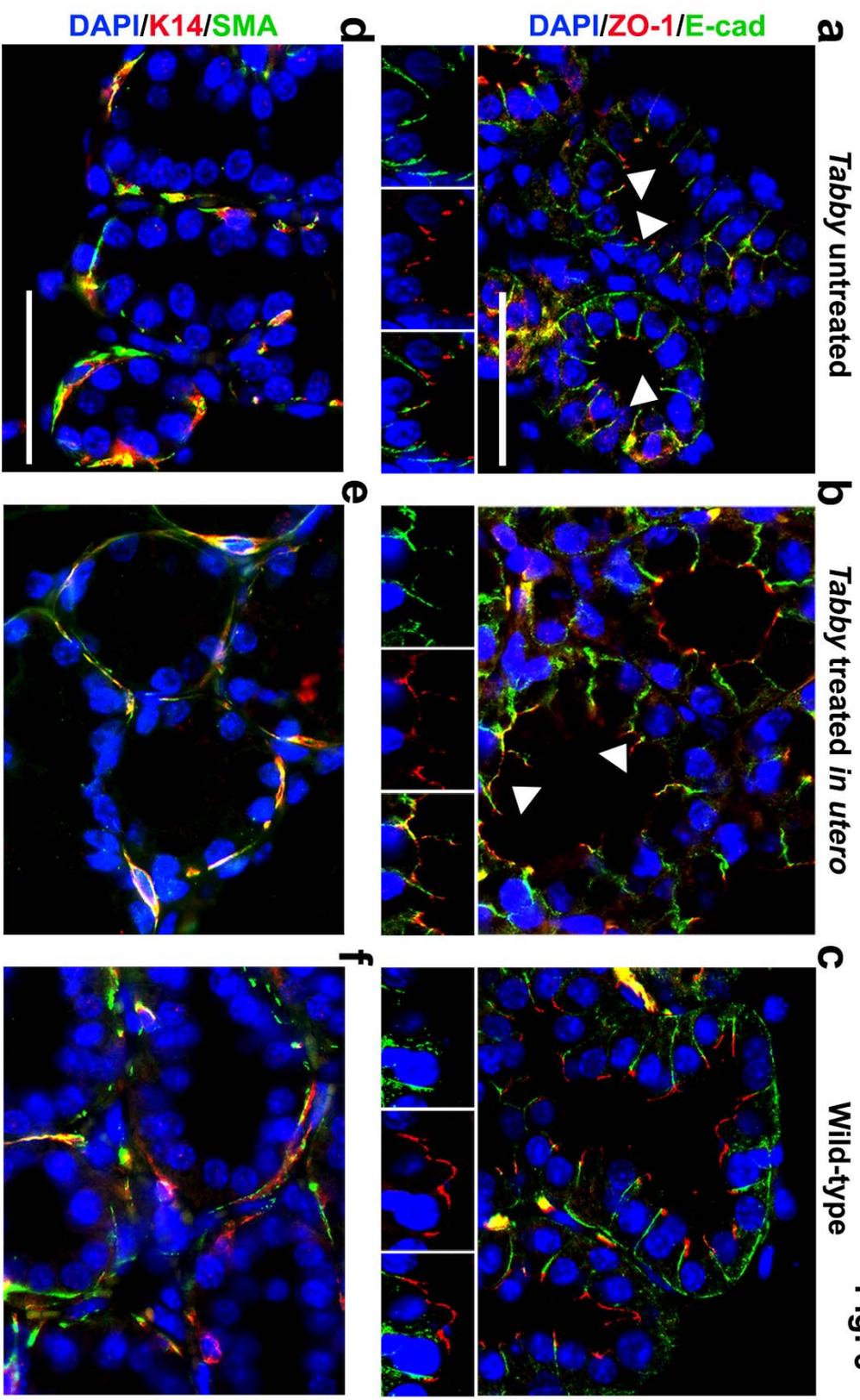
Fig. 7
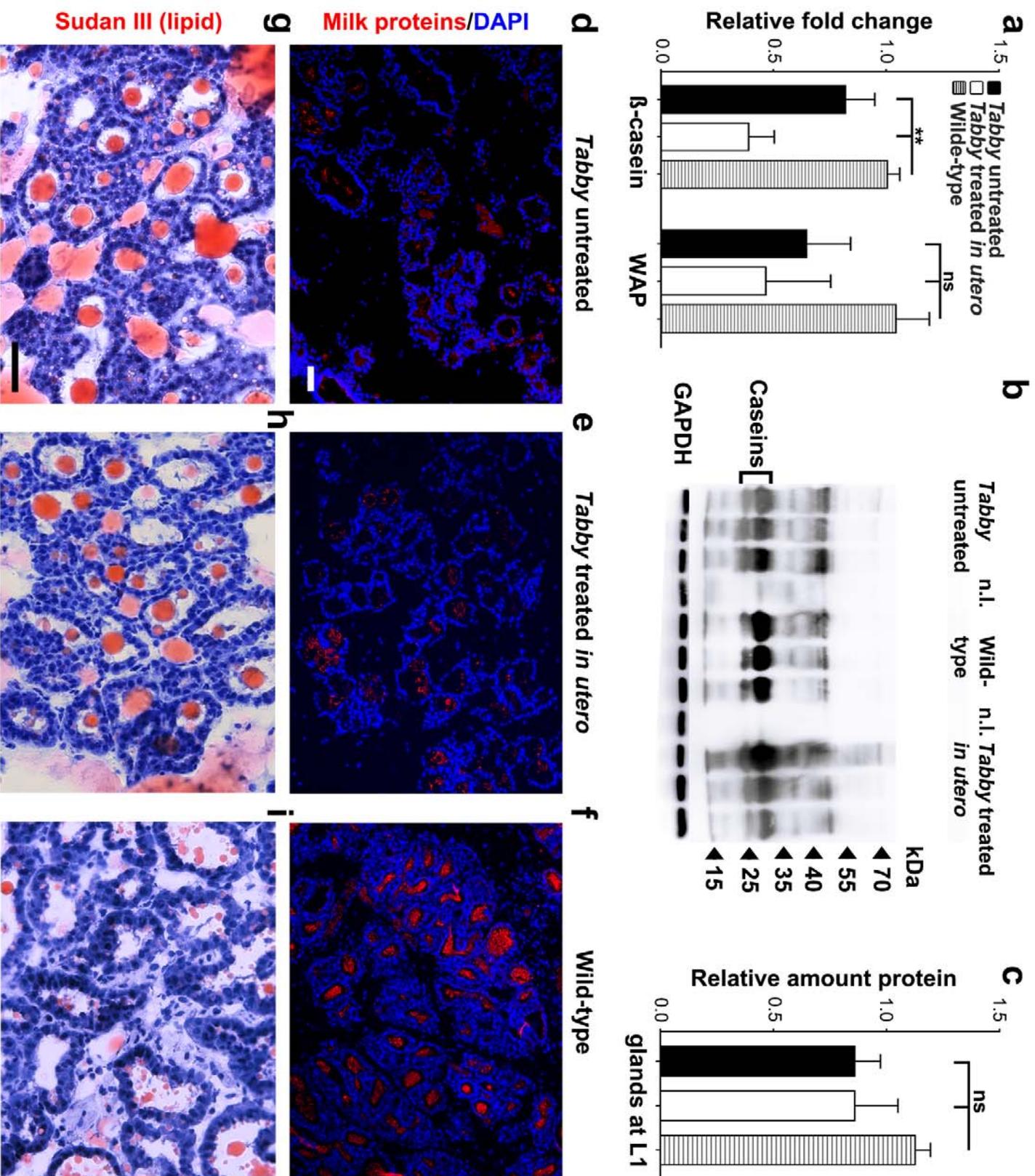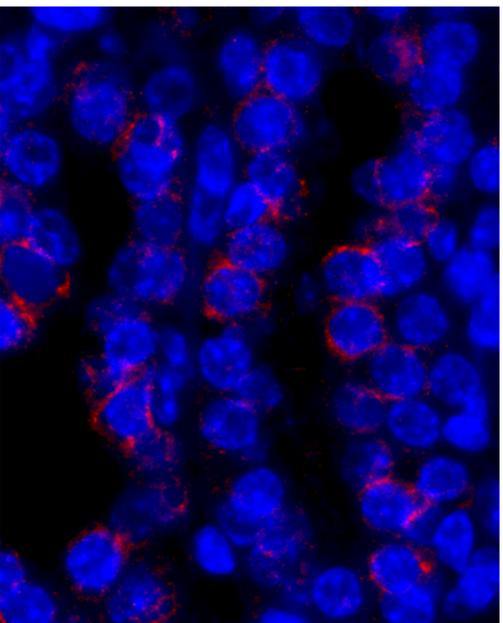
Fig. S1
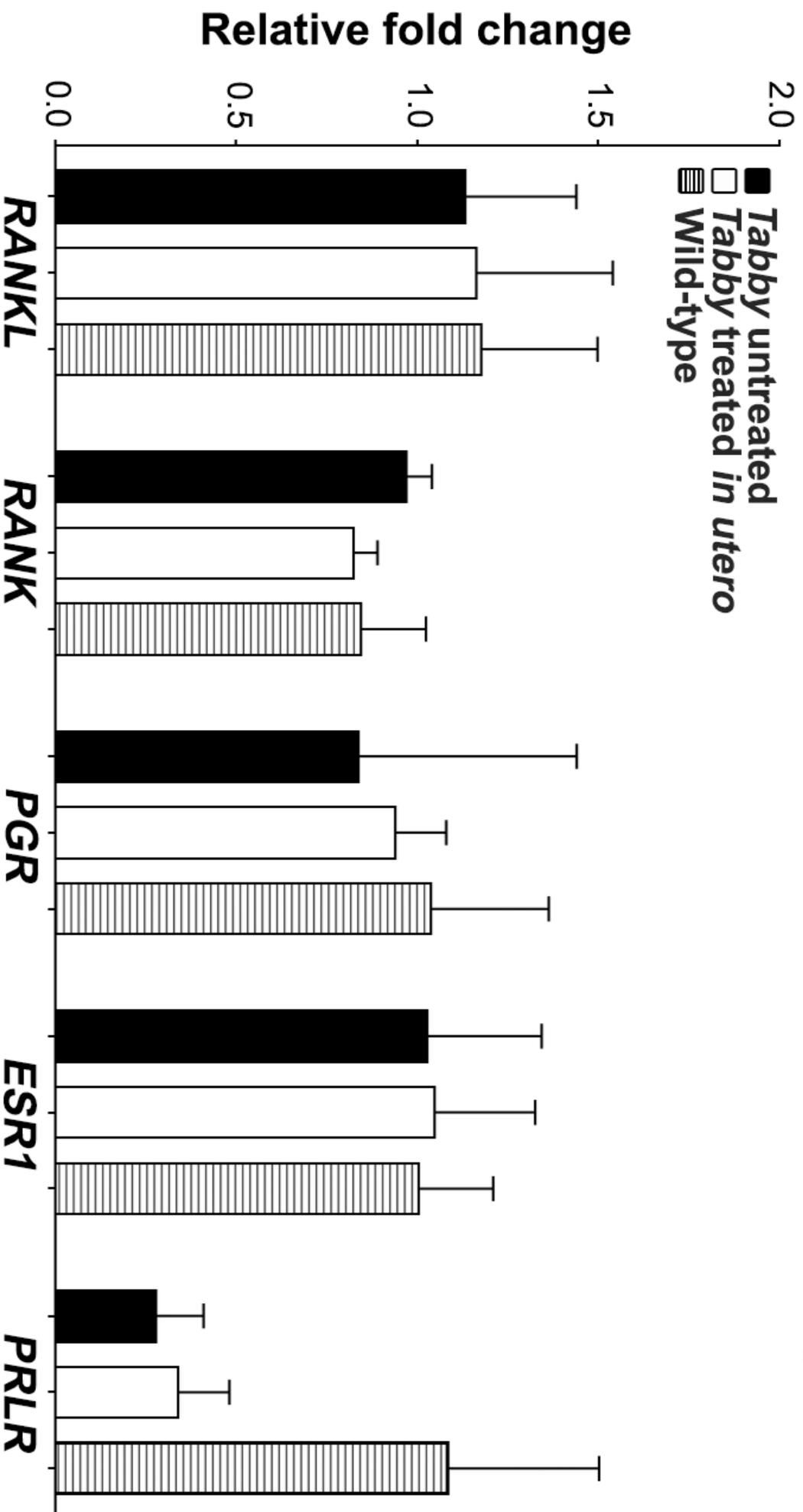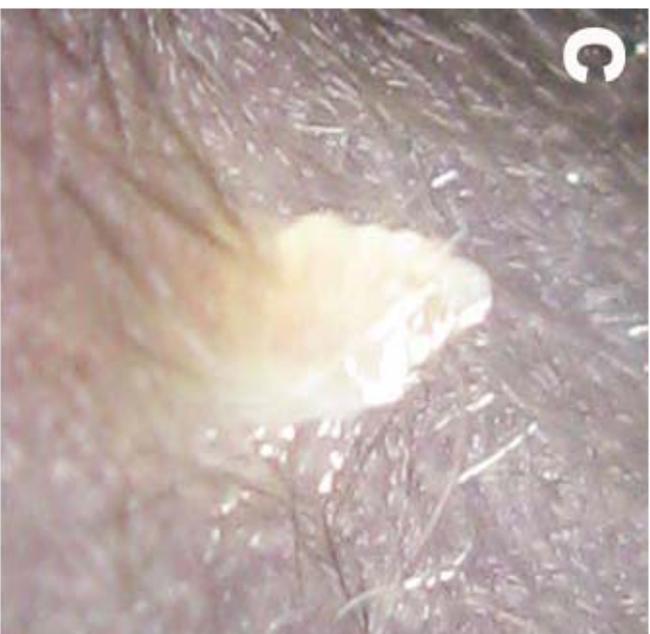
Fig. S2

DAPI/Occludin

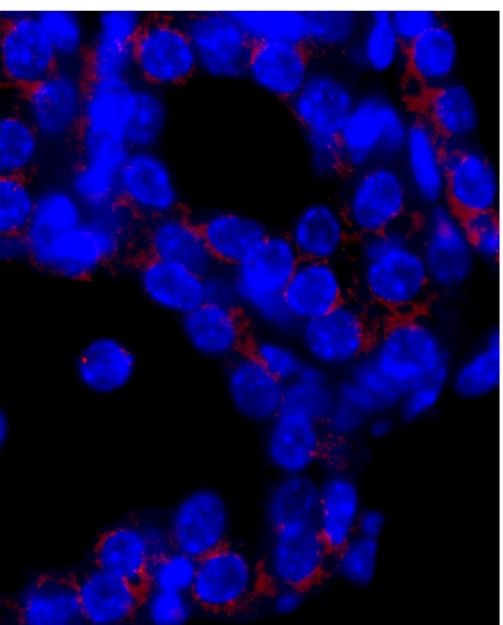a   *Tabby untreated*

b   *Tabby treated in utero*

c   Wild-type

Fig. S3